UNIVERSITY OF CALIFORNIA, SAN DIEGO

Functional and Morphological Changes in a Rat Model of Knee Osteoarthritis

A Thesis submitted in partial satisfaction of the requirements for the degree Master of Science

in

Biology

by

Kevin Cheng

Committee in charge:

Professor Koichi Masuda, Chair
Professor Kimberly Cooper, Co-Chair
Professor James Posakony

2017

The Thesis of Kevin Cheng is approved and it is acceptable in quality and form for publication on microfilm and electronically:

Co-Chair

Chair

University of California, San Diego

2017

TABLE OF CONTENTS

LIST OF ABBREVIATIONS

ACL	Anterior cruciate ligament
ACLT	Anterior cruciate ligament transection
BMD	Bone mineral density
BS/TV	Bone surface density
BV/TV	Percent bone volume
HA	Hyaluronic acid, or referring in this thesis to the pharmaceutical injection or the treatment group.
HLWD	Hind limb weight distribution
MCL	Medial collateral ligament
MMT	Medial meniscus transection
OA	Osteoarthritis
OARSI	Osteoarthritis Research Society International
PBS	Phosphate buffered saline, or referring in this thesis to the solution or the treatment group.
pMMT	Partial medial meniscus transection
PTOA	Post-traumatic osteoarthritis
Tb.N	Trabecular number
Tb.Sp	Trabecular separation
Tb.Th	Trabecular thickness

LIST OF FIGURES

LIST OF TABLES

ACKNOWLEDGEMENTS

I would like to acknowledge Professor Koichi Masuda for his support and guidance, not only as the chair of my committee, but also as my mentor during my five years of investigating spine and knee orthopedics in his laboratory. The knowledge, opportunities, and experiences that I gained from working with Dr. Masuda have proven and will continue to prove to be invaluable in my academic pursuits.

I would also like to acknowledge Kenji Kato, Shingo Miyazaki, and Junichi Yamada of the Skeletal Translational Research Laboratory in the Department of Orthopaedic Surgery at UCSD as co-authors for their indispensable help on the work presented in this thesis. The presented study may be prepared for publication in the future. Kevin Cheng was the primary investigator and author of this study.

ABSTRACT OF THE THESIS

Functional and Morphological Changes in a Rat Model of Knee Osteoarthritis

by

Kevin Cheng

Master of Science in Biology

University of California, San Diego, 2017

Professor Koichi Masuda, Chair
Professor Kimberly Cooper, Co-Chair

In the United States, the estimated lifetime risk of developing knee osteoarthritis is approximately 44%. Therefore, animal models are necessary to study the etiology of the disease as well as the efficacy of therapeutic treatments. In this study, a combination of anterior cruciate ligament transection (ACLT) and partial medial meniscal transection (pMMT) was performed on rat knees to investigate changes in behavior, cartilage, and bone morphology due to post-traumatic osteoarthritis (PTOA). Hyaluronic acid (HA) intra-articular injection was administered to the knee one week after the surgeries. ACLT +

pMMT surgery resulted in a temporary contralateral preference in static weight bearing, minor degeneration of the articular cartilage, and generally decreased bone quality. However, among the parameters analyzed, the most sensitive parameter for characterizing PTOA changes in the ACLT + pMMT model was trabecular thickness from μCT analyses. Treatment with HA was also found to attenuate the progression of PTOA changes in articular cartilage and bone morphology.

1. INTRODUCTION

Osteoarthritis is the most common joint disease in the United States (1, 2). Of all the chronic degenerative joint diseases, knee osteoarthritis (OA) is the most common in the United States, with an estimated lifetime risk of 40% in men and 47% in women (3, 4). Ultimately, OA results in disability, economic loss, and lowered quality of life (5).

The knee joint is comprised of the distal femur and proximal tibia. Coating the ends of these bones is articular cartilage, a thin layer of connective tissue composed of chondrocytes and extracellular matrices made up of glycosaminoglycans and collagen that function to reduce friction in the movement of the joint. Several ligaments are also located within the knee, such as the anterior cruciate ligament (ACL), medial collateral ligament (MCL), posterior cruciate ligament, and lateral collateral ligament, all functioning to stabilize the joint. The entire knee joint is enveloped by a synovial membrane, which keeps synovial fluid within the joint. Synovial fluid, which is rich in hyaluronic acid, functions to reduce friction in the movement of the joint by providing cushioning and lubricating properties in conjunction with the articular cartilage on the surface of the distal femur and proximal tibia (6, 7).

The clinical presentation of OA is typically pain and functional disability (8-10). Although the exact etiology of OA has not yet been elucidated, it is known that OA is a whole-joint disease (10). In OA disease, the articular cartilage can break down due to trauma or the release of catabolic enzymes, such as matrix metalloproteinases (MMPs) (11, 12). Because of the cartilage degeneration, a redistribution of loading occurs in the knee, causing the formation of osteophytes as well as bone changes, such as thickening of the

subchondral and trabecular bone (10, 11, 13, 14). Additionally, the synovial membrane can become inflamed, resulting in the upregulation of pro-inflammatory cytokines, such as IL-1β and TNFα, which further amplify catabolic processes within the joint (15, 16). The concentration of hyaluronic acid in the synovial fluid has also been reported to decrease in OA disease (17, 18).

There currently exists non-pharmacological and pharmacological treatments of OA with varying evidences of efficacy. Non-pharmacological treatments of OA include aerobic exercises, heating and icing of the joint, strength training, weight reduction, and knee braces (19). Current pharmacological treatments for OA include acetaminophen, nonsteroidal anti-inflammatory drugs (NSAIDs), COX-2 inhibitors, oestrogen, and intra-articular injections of corticosteroids and hyaluronic acid (19, 20). There is no conclusive agreement on the administration of some treatments among clinicians and researchers because of mixed conclusions on treatment efficacies in clinical settings. For example, despite much literature documenting the positive efficacy of intra-articular hyaluronic acid injections (17, 18, 21-28), the American Academy of Orthopedic Surgeons (AAOS) maintains a strong recommendation against the use of hyaluronic acid for knee OA patients because of inconclusive clinical evidence (29). In general, however, current treatments target only the symptoms of OA (i.e., pain and joint stiffness) and do not directly modify the disease to restore the changes caused by the disease. To date, a disease-modifying drug for OA has not been found (19, 20).

To study the etiology of knee OA, as well as the efficacy of potential pharmacologic therapeutics, animal disease models are required. There have been many animal species used to study OA, including mouse, rat, rabbit, and guinea pig (**Table 1**) (30-32). Selection

of an animal model requires the consideration of factors, such as the size of the knee joint, thickness of the articular cartilage, postoperative management, joint loading, cost, as well as public perception (30).

Table 1: Summary of animal species and methods of OA induction utilized in knee OA studies (30-32).

Species	Induction	Factors to consider
• Mouse • Rat • Rabbit • Guinea pig • Dog • Sheep • Goat • Horse	• Chemical injection (ie. catabolic enzymes, monoiodoacetate) • Surgery ▪ ACL transection (ACLT) ▪ Medial meniscus transection (MMT) ▪ Destabilization of medial meniscus (DMM) • Impact loading • Immobilization • Spontaneous OA (dog, guinea pig, horse)	• Size of knee joint • Postoperative management • Pain assessment • Joint loading • Cost • Public perception

Similarly, there are many different methods of OA induction, including chemical injection, impact loading, immobilization, and surgery (**Table 1**) (30, 32). Spontaneous OA can occur in some animals, such as dogs, guinea pigs, and horses; however, this progression of OA is slow and may not be consistent among animals within studies (32). Selecting the method of OA induction to be used is important and requires the consideration of the mechanism of OA progression desired. For example, the use of monoiodoacetate (MIA) injection to induce OA differs from surgically-induced models of OA because MIA only chemically causes chondrocyte death and is, therefore, only able to mimic biochemical changes and not the biomechanical changes that are relevant to the disease as well (11, 33). There are also differences in the mechanism and length of OA progression among surgically-induced models, such as patellectomy, anterior cruciate

ligament transection, medial meniscal tear, partial medial meniscal transection, and medial collateral ligament transection (32). When selecting the animal species and method of OA induction for a study, these factors need to be considered so that the experimental hypothesis can be appropriately addressed. For example, MIA injection to induce OA would only be appropriate for studying OA pain, but not the efficacy of regenerative therapeutics because MIA would likely cause cartilage degeneration too severe for any regenerative potential to remain.

For our study, the rat model of OA was selected because of its thicker articular cartilage (compared to mice) and lower cost (compared to rabbits) (30). Additionally, a rat OA model allows for the pain and behavior tests that are not feasible in rabbits. The method of OA induction selected was to surgically induce OA by a combination of ACL transection (ACLT) and partial medial meniscal transection (pMMT). Gerwin et al. reported that ACLT + pMMT in mature rats causes progressive cartilage degeneration that is slower than medial meniscal transection only, but faster and more severe than ACLT only, resulting in a more representative progression of OA disease (33). Because a surgical model of OA induction was used, the findings reported in this study are more relevant to OA caused by physical injury, such as ACL tears or other forms of trauma (post-traumatic OA, PTOA) compared to spontaneous or idiopathic OA.

Because behavioral, histological, and bone morphological data are commonly obtained in OA pharmacological efficacy studies, it is important to characterize these measurements in an OA model as to establish baseline measurements for those parameters. Bagi et al. previously reported correlations between micro-computed tomography (μCT) imaging, histology, and functional capacity in the medial meniscal tear rat model of OA

(34). However, preliminary studies performed utilizing minimally invasive surgical techniques within our laboratory suggest that a combined ACLT and pMMT model of OA results in a milder, but detectable progression of PTOA disease, compared to ACLT and MMT surgeries by themselves. Therefore, it is important to characterize the changes in histological grading, behavioral analyses, and μCT quantifications in the ACLT + pMMT rat model of OA. In addition, a current clinical standard for OA disease management, an intra-articular injection of a high molecular weight hyaluronic acid (hylan G-F 20), was administered to a group of animals to establish baseline measurements for the changes observed resulting from this method of OA treatment (21, 28, 35, 36). We hypothesized that 1) the ACLT + pMMT procedure will induce functional and bone changes characteristic of PTOA, 2) intra-articular injections of hyaluronic acid will attenuate early PTOA changes in cartilage and bone, and 3) one outcome measure can be identified as the most sensitive parameter for characterizing PTOA changes among the multiple outcome measures obtained in this study.

2. METHODS

2.1: Animals

Institutional Animal Care and Use Committee (IACUC) approval was obtained for all *in vivo* procedures (Protocol: S08294). Male 9-10 weeks-old Wistar rats (Harlan Laboratories, Indianapolis, IN, USA) weighing approximately 330 g were used for this study. A total of 24 rats were split equally among 3 groups: hyaluronic acid injection (HA), PBS injection (PBS) and sham groups. At 0W of the study, there was a significantly higher average body weight in the PBS (365.6 g, $p<0.0001$) and HA (355.1 g, $p<0.0001$) groups when compared to that of the Sham group (267.5 g). However, at 9W of the study, there were no significant differences in body weight among the groups ($p=0.1508$). On average, there was a 133 g weight gain among all animals in the study.

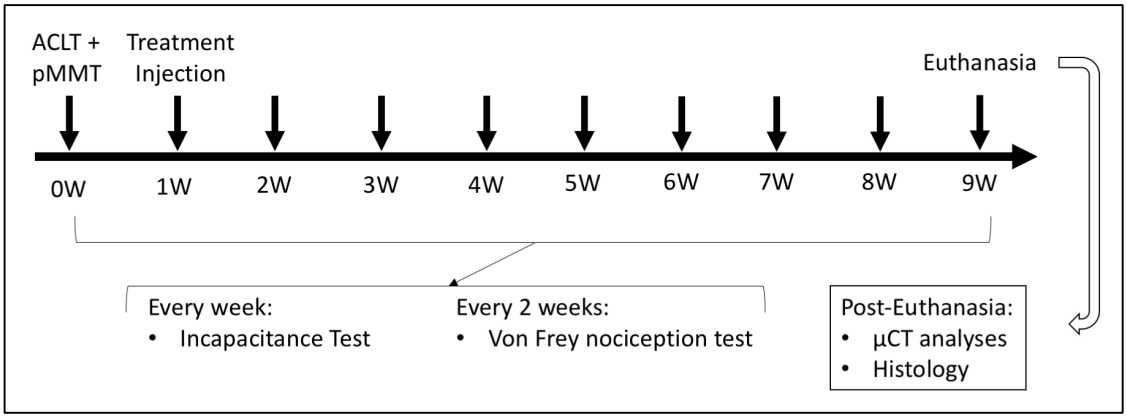

Figure 1: Summary of the experimental timeline. ACLT and pMMT procedures were performed at 0W, and treatment injections (PBS or HA) were administered at 1W. Incapacitance testing was performed every week of the study, whereas Von Frey testing was performed every 2 weeks after 2W. µCT and histological analyses were performed after euthanasia of the animals.

2.2: Surgery

General anesthesia was induced by an intramuscular injection of a mixture of ketamine (75 mg/kg, Zetamine®; VETone, Boise ID, USA), xylazine (3 mg/kg, AnaSed®; LLOYD Laboratories, Shenandoah, IA, USA), and buprenorphine (0.03 mg/kg, Buprenex®; Reckitt Benckiser Pharmaceuticals, Richmond, VA, USA) for sedation and analgesia prior to the surgery. Isoflurane inhalation (3%) was used to maintain anesthesia. Surgical procedures were performed only on the right knee, leaving the left knee as an unoperated contralateral control. The knee was shaved and prepared antiseptically. For the HA and PBS groups, a 3 cm paramedian incision was made from the distal patella toward the proximal tibial plateau. The joint capsule immediately medial to the patellar tendon was incised and opened. Blunt dissection of the fat pad over the intercondylar area was then performed to expose the intercondylar region to provide visualization of the anterior cruciate ligament (ACL). The patella was dislocated laterally to give a greater exposure of the femorotibial joint. The ACL and the anterior half of the medial meniscus were transected (ACLT + pMMT). The patella was then replaced, and the fascia and subcutaneous layer were sutured using 4-0 absorbable sutures and surgical glue was applied to the incision site. The Sham group received the same surgical exposure without transection of the ACL and medial meniscus.

2.3: Knee Injections

One week following surgery, animals in the HA group received a 50 μL intra-articular injection of high molecular weight hyaluronic acid (hylan G-F 20, Synvisc®; Genzyme Corporation, Cambridge, MA, USA) in the right knee joint. Animals in the PBS

group received a 50 µL intra-articular injection of phosphate-buffered saline. Contralateral knees were not injected. Sham group animals were also not injected.

2.4: Von Frey Nociception Test

The Von Frey nociception test has been reported as a method for measuring mechanical nociception in rodents (37, 38). Specifically, the Von Frey test has been reported as a method for quantifying pain due to OA (39, 40). The Von Frey test was performed on the rats at 1 week after the surgery and at every 2 weeks from that point onwards. Rats were placed on a suspended wire mesh which allowed for full access to the hind paws. Rats were first placed on the wire mesh for 20 minutes before testing at each time point to allow for rats to acclimate to the environment. Von Frey filaments of different stiffness (4.31, 4.56, 4.74, 4.93, and 5.18 g) were incrementally applied perpendicular to the center of the plantar surface of each hind paw for 6-8 seconds. A positive response was recorded when a rapid paw withdrawal was observed in response to the filament presentation. Using the up-down method, 50% paw withdrawal threshold was determined as described by Chaplan et al. (41, 42).

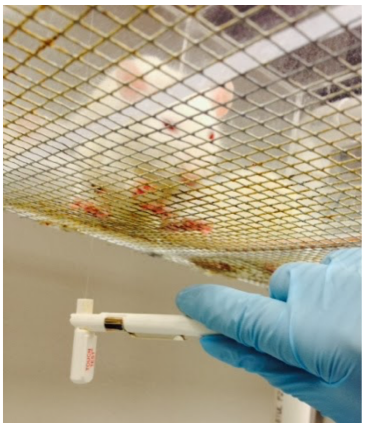

Figure 2: Von Frey nociception test was performed on rats to assess mechanical nociception after ACLT + pMMT surgery.

2.5: Incapacitance Test

Incapacitance testing has been reported as an assessment of inflammation or pain in the hind limbs by measuring static weight bearing (43, 44). For every week of the study, static weight bearing of the hind limbs was tested using an Incapacitance Tester (Columbus Instruments, Columbus, OH, USA). Two sensors on the machine independently measure the weight loaded on the left and right hind limbs. To limit the variation in measurements due to the position and posture of the rat within the incapacitance chamber, measurements are taken only when (i) the rat is stationary, (ii) the left and right hind paws are aligned at the same position on each sensor, and (iii) the left and right front paws are placed at the same position on the chamber wall so that one paw is not above the other. The force applied by each hind limb was averaged over a 5 second period. For each animal at each time point, 10 measurements were obtained. Hind limb weight distribution (HLWD) was expressed relative to the right hind limb as a percentage of the total weight applied by both hind limbs by dividing the weight exerted by the right hind limb by the sum of the weights of both right and left hind limbs (Right / Right + Left). The percentages of all 10 measurements at each time point were then averaged for each animal.

Figure 3: Static weight bearing was tested by using an incapacitance tester to assess inflammation or pain in the hind limbs following ACLT + pMMT surgery.

2.6: Sample Collection

At 9 weeks after surgery, animals were euthanized. For both left and right sides, the entire knee joint was harvested and stored in 10% formalin for histological and μCT bone analyses.

2.7: Micro-Computed Tomography (μCT) Scanning and Analyses

μCT scanning was performed for three-dimensional (3D) bone morphological analyses. Left and right knee joints were μCT scanned with a Skyscan 1076 μCT scanner (Bruker, Kontich, Belgium) at a 9 μm resolution, 70 kV, 142 μA, using a 1.0 mm aluminum filter with an average scan time of 1 hour per knee joint. Knees were wrapped in formalin-soaked gauze and placed in 50 mL conical tubes for scanning. The scanning region was selected such that the distal femoral epiphysis and metaphysis and the proximal tibial epiphysis and metaphysis were included in the scan for bone morphological analyses. Hydroxyapatite phantom rods (4 mm diameter; 0.25 and 0.75 g/cm^3) were scanned with the samples for bone mineral density (BMD) calibration and analyses.

Reconstructed transaxial bitmap image files for each scan were first opened using Dataviewer software (Bruker, Kontich, Belgium) to rotate the scans to align the femur, tibia, and joint space with the transaxial, coronal, and sagittal planes. Then, the rotated datasets were opened in CT-Analyser (Bruker, Kontich, Belgium) to select the regions of interest (ROI) for analysis. Four ROIs were manually selected for each knee for individual analysis of the femur epiphysis, femur metaphysis, tibia epiphysis, and tibia metaphysis (**Figure 4**). ROIs were carefully drawn to include only the trabecular bone and to exclude the cortical bone. For the femur, the epiphysis was defined as any trabecular bone distal to the epiphyseal plate and the metaphysis was defined as any trabecular bone within 4 mm

proximal from the epiphyseal plate. For the tibia, the epiphysis was defined as any trabecular bone proximal to the epiphyseal plate and the metaphysis was defined as any trabecular bone within 4 mm distal from the epiphyseal plate. Using CT-Analyser, all 4 ROIs for each knee sample were analyzed for the following parameters: bone mineral density (BMD), trabecular thickness (Tb.Th), trabecular number (Tb.N), trabecular separation (Tb.Sp), percent bone volume (BV/TV), and bone surface density (BS/TV) (45).

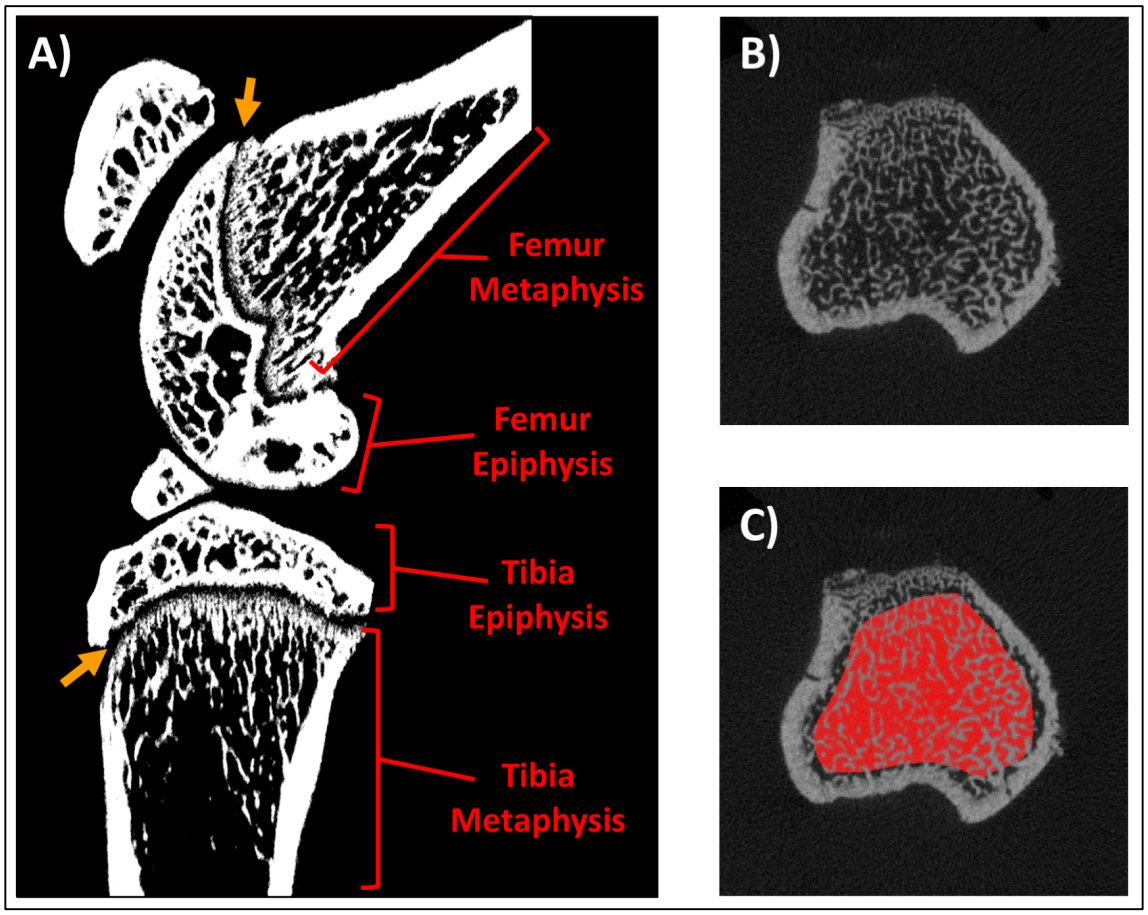

Figure 4: A) Four bone segments (femur metaphysis, femur epiphysis, tibia epiphysis, tibia metaphysis) were manually selected for bone morphological analyses. The epiphyseal plates are indicated by the arrows. **B)** A transaxial µCT slice of a tibia metaphysis before and **C)** after ROI selection (shown in red). ROI were manually selected as to include only trabecular bone and to avoid cortical bone.

2.8: Histology

After µCT scanning, knee samples were prepared for histological analyses. Knee samples were decalcified using a solution containing 7% formalin and 10% formic acid (Cal-Ex II; Fischer Scientific, Hampton, NH). After decalcification, knee samples were embedded in paraffin, and coronal sections were made to visualize the medial tibial plateau (MTP) of the tibial articular cartilage. The slices then were stained with safranin-O to detect

the glycosaminoglycan content of the MTP cartilage. Slides were scanned at 40X objective using a Leica SCN400 Slide Scanner (Leica, Wetzlar, Germany).

Histological scoring of the MTP for OA degeneration was performed using the Osteoarthritis Research Society International (OARSI) scoring system as reported by Pritzker et al. (46). The OARSI score is dependent on two histopathological assessments: grade and stage. The histopathology grade assessment is dependent on the morphological features of the articular cartilage due to OA, such as surface irregularities, cell death, cartilage matrix loss, and decreased Safranin O staining with grades ranging from 0 to 6 **(Table 2)**. The histopathology stage assessment ranges from stage 0 to 4, depending on the percentage of the total surface or area affected by the OA changes **(Table 3)**. If no changes in structure or morphology are observed, then a stage of 0 is assigned. If more than 50% of the total surface or area is affected by OA changes, then a stage of 4 is assigned. The final OARSI score is obtained by multiplying the grade and stage assessments, resulting in scores ranging from 0-24, with 24 representing the most severe OA cartilage degeneration. Histological scoring was performed by two independent observers and the inter-observer agreement was calculated.

Table 2: OARSI score histopathological grade assessment as reported by Pritzker et al.(46).

Grade (Key Feature)	Subgrade
Grade 0: Surface intact, cartilage intact	No subgrade
Grade 1: Surface intact, but uneven.	1.0: Cells intact
	1.5: Cell death
Grade 2: Surface discontinuity	2.0: Fibrillation through superficial zone
	2.5: Surface abrasion with matrix loss within superficial zone
Grade 3: Vertical fissures	3.0: Simple fissures
	3.5: Branched/complex fissures
Grade 4: Erosion	4.0: Superficial zone delamination
	4.5: Mid zone evacuation
Grade 5: Denudation	5.0: Bone surface intact
	5.5: Reparative tissue surface present
Grade 6: Deformation	6.0: Joint margin osteophytes
	6.5: Joint margin and central osteophytes

Table 3: OARSI score histopathological stage assessment as reported by Pritzker et al.(46).

Stage	% Involvement (surface, area)
Stage 0	No OA activity seen
Stage 1	<10%
Stage 2	10-25%
Stage 3	25-50%
Stage 4	>50%

2.9: Statistics

All statistical analyses were performed using GraphPad Prism 7.0 (GraphPad, La Jolla, CA, USA). Two-way ANOVA tests were performed to test for significant effects of time and treatment. One-way ANOVA tests were performed to test for significant effects

of treatment. Fisher's PLSD post hoc tests were performed to find significant differences due to multiple comparisons. A Mann-Whitney U test was performed to test for significant differences between PBS and HA histology scores. All values are displayed as mean ± standard error.

3. RESULTS

3.1: Von Frey Nociception

All animals were tested for nociceptive pain using Von Frey filaments at 1 week after surgery, at 1 week after injection treatments, and at every 2 weeks afterward until the end of the 9-week study. At 0W, all animals had a 50% paw withdrawal threshold of 15 g. The only significant differences among all groups at all time points was observed at 1W, where a significant decrease in 50% paw withdrawal threshold was observed in the PBS ($p<0.01$) and HA ($p<0.01$) groups when compared to that of the Sham group (**Figure 5**). By 8W, all groups had returned to a 15 g 50% paw withdrawal threshold.

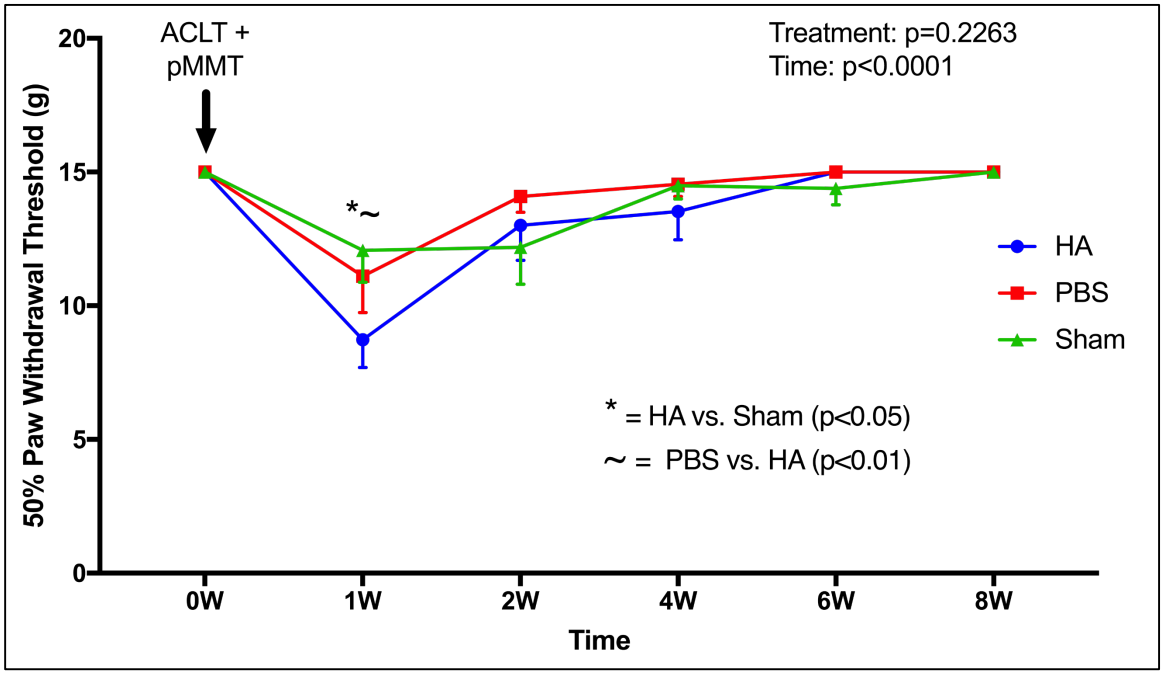

Figure 5: Von Frey nociception test. 50% paw withdrawal threshold was determined using the up-down method (41). Significant differences were observed between Sham and HA ($p<0.05$) and PBS and HA ($p<0.01$) only at 1 week after the surgery, before the intra-articular injection treatments. No significant differences among groups were observed at any other time points. There was a significant effect of time ($p<0.0001$), but not treatment ($p=0.2263$).

3.2: Incapacitance

Incapacitance testing to assess changes in static weight bearing was performed prior to the surgery and weekly postoperatively. Hind limb weight distribution (HLWD) was expressed relative to the right hind limb as a percentage of the total weight applied by both hind limbs. A two-way ANOVA found both time and treatment to have significant effects on HLWD ($p<0.0001$). Before the surgery, HLWD was 50.1% in all animals in all groups (**Figure 6**). At one week after the surgery before treatment injections were administered, HLWD in the HA (40.5%) and PBS (38.4%) groups were significantly lower than that of the Sham group (48.9%, $p<0.01$). After the treatment injections were administered, HLWD of the HA and PBS groups were still significantly lower than that of the Sham group ($p<0.01$); however, no significant differences were observed among groups from 4 weeks post-surgery to the end of the study.

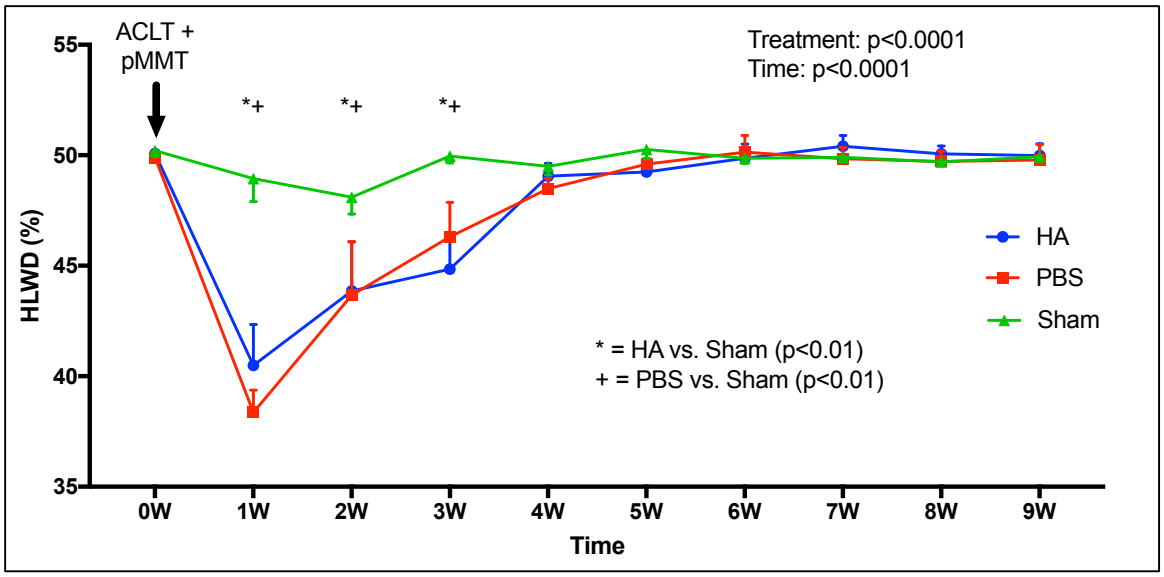

Figure 6: Hind limb weight distribution (HLWD) for all 3 treatment groups at every time point is shown. HLWD is expressed relative to the right hind limb as a percentage of the total weight applied by both hind limbs by dividing the weight exerted by the right hind limb by the sum of the weights of both right and left hind limbs. The HA ($p<0.01$) and PBS ($p<0.01$) groups had significantly lower HLWD compared to the Sham group at 1W, 2W, and 3W time points. No other significant differences among groups were observed at any other time points.

3.3: Histological Analyses

Coronal sections of the MTP were stained with safranin-O and scored using the OARSI score as described by Pritzker et al. (46). Histological scoring was performed only for the PBS and HA groups, as the histological processing of the Sham group samples is ongoing. Because the majority of the cartilage defects were not severe, much attention was given to observe small changes, such as cell death or cell clustering, in the MTP that would indicate OA changes. Samples receiving an OARSI score of 0 generally had normal articular cartilage, with smooth cartilage surface, clear layered organization of matrix and chondrocytes, and retention of Safranin-O staining (**Figure 7A)**. Samples receiving higher OARSI scores were observed to have cell death, superficial fibrillation of the matrix, depletion of Safranin-O staining, and vertical fissures. The inter-class reliability coefficient

from the scores of two independent observers was 0.943. There were no statistical differences found between mean scores of the PBS and HA groups (p=0.6298, **Figure 7B**). However, OARSI scores in the PBS group tended to have a higher variation than that of the HA group. In the PBS group, the highest OARSI score received by one sample was 9.0, whereas the highest score received in the HA group was 5.0.

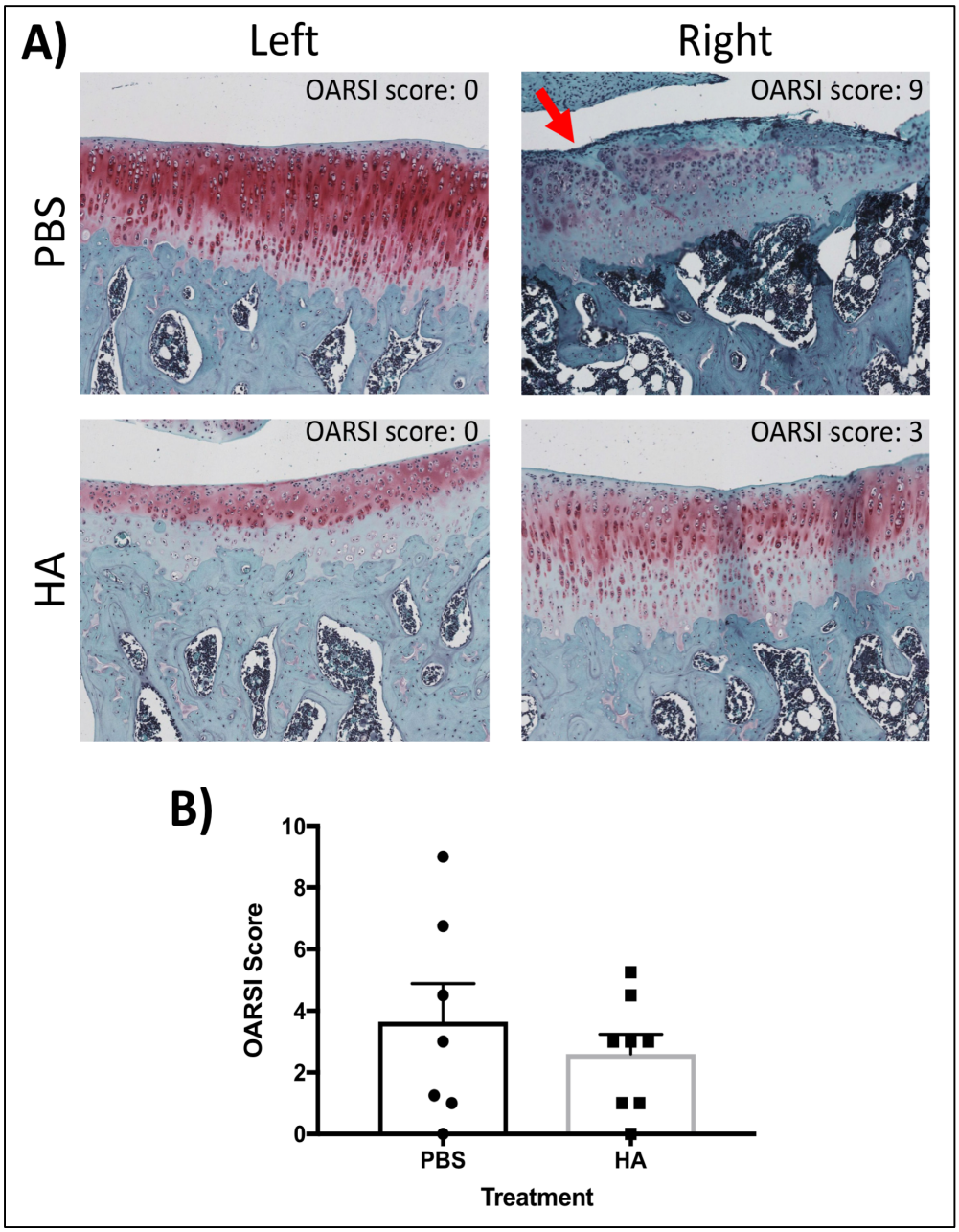

Figure 7: A) Histology of the coronal sections of the medial tibial plateau (MTP) from the PBS and HA groups. Sections were stained with safranin-O. The left MTP samples show normal articular cartilage, with smooth cartilage surface, layered organization of matrix and chondrocytes, and retention of Safranin-O staining (red). The right MTP samples show cell death, superficial fibrillation of the matrix, depletion of Safranin-O staining, and a fissure (PBS, Right, indicated by the arrow). The OARSI score assigned for each sample shown is indicated. **B)** Average OARSI scores of PBS and HA groups. Dots indicate scores of individual samples. Although MTP samples from the PBS group tended to have higher OARSI scores when compared to those of the HA group, a Mann-Whitney U test found no significant differences between the two groups ($p=0.6298$).

3.4: μCT Analyses

Data for the μCT analyses are represented as absolute values as well as normalized values (Right/Left). Data are represented as normalized values because the differences between right and left knees within the same animal were larger than differences among treatment groups in some parameters. There were no significant differences in measurements among left, contralateral knees of different treatment groups for trabecular thickness ($p=0.1331$), trabecular separation ($p=0.3136$), percent bone volume ($p=0.8302$), and bone surface density ($p=0.1262$), although significant differences were observed for bone mineral density ($p=0.0002$) and trabecular number ($p<0.0001$). Three animals from the PBS group were excluded from μCT analyses because of abnormal ring artifacts in the scan images.

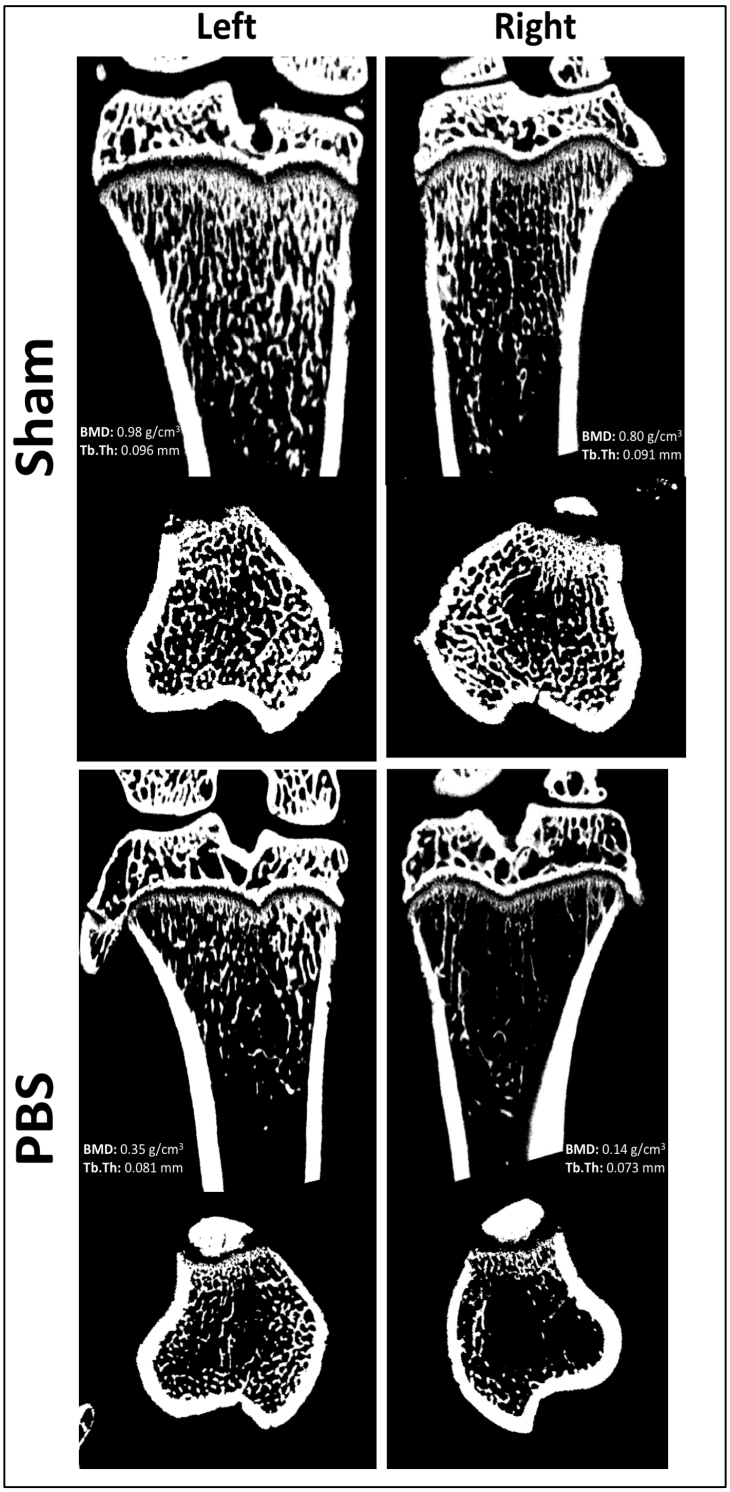

Figure 8: Representative coronal and transaxial cross-sections of tibias from the Sham and PBS groups 9 weeks after ACLT + pMMT. Upon visual inspection, there are no remarkable differences between the left and right tibias in the Sham group. However, the right tibia appears to have decreased bone mass compared to the left tibia in the PBS group. Bone mineral density (BMD) and trabecular thickness (Tb.Th) values the samples are shown.

3.4.1: Bone Mineral Density

In general, absolute bone mineral density (BMD) in the Sham group was higher than both PBS and HA groups in all bone segments analyzed. Significant effects of treatment on BMD were found in the femur epiphysis, femur metaphysis, and tibia epiphysis ($p<0.001$ for all) but not in the tibia metaphysis ($p=0.1387$). In the femur epiphysis, femur metaphysis, and tibia epiphysis, BMD of the Sham group was significantly higher than that of the PBS and HA groups ($p<0.01$ for all, **Figure 9**). In the femur metaphysis, BMD of the Sham, PBS, and HA groups was found to be 1.1070, 0.5766, and 0.6999 g/cm^3, respectively. In the tibia epiphysis, BMD of the Sham, PBS, and HA groups was found to be 1.4660, 0.8184, and 0.9489 g/cm^3, respectively. The HA group also tended to have a higher BMD compared to the PBS group at all bone segments, although no significant differences were found.

When BMD was normalized to the contralateral controls, significant differences were only found between Sham/PBS and HA/PBS in the femur metaphysis and between Sham/PBS in the tibia epiphysis ($p<0.05$ for all), although no significant effect of treatment was found (**Figure 9**). No significant differences were found between Sham and HA groups at any bone segment analyzed.

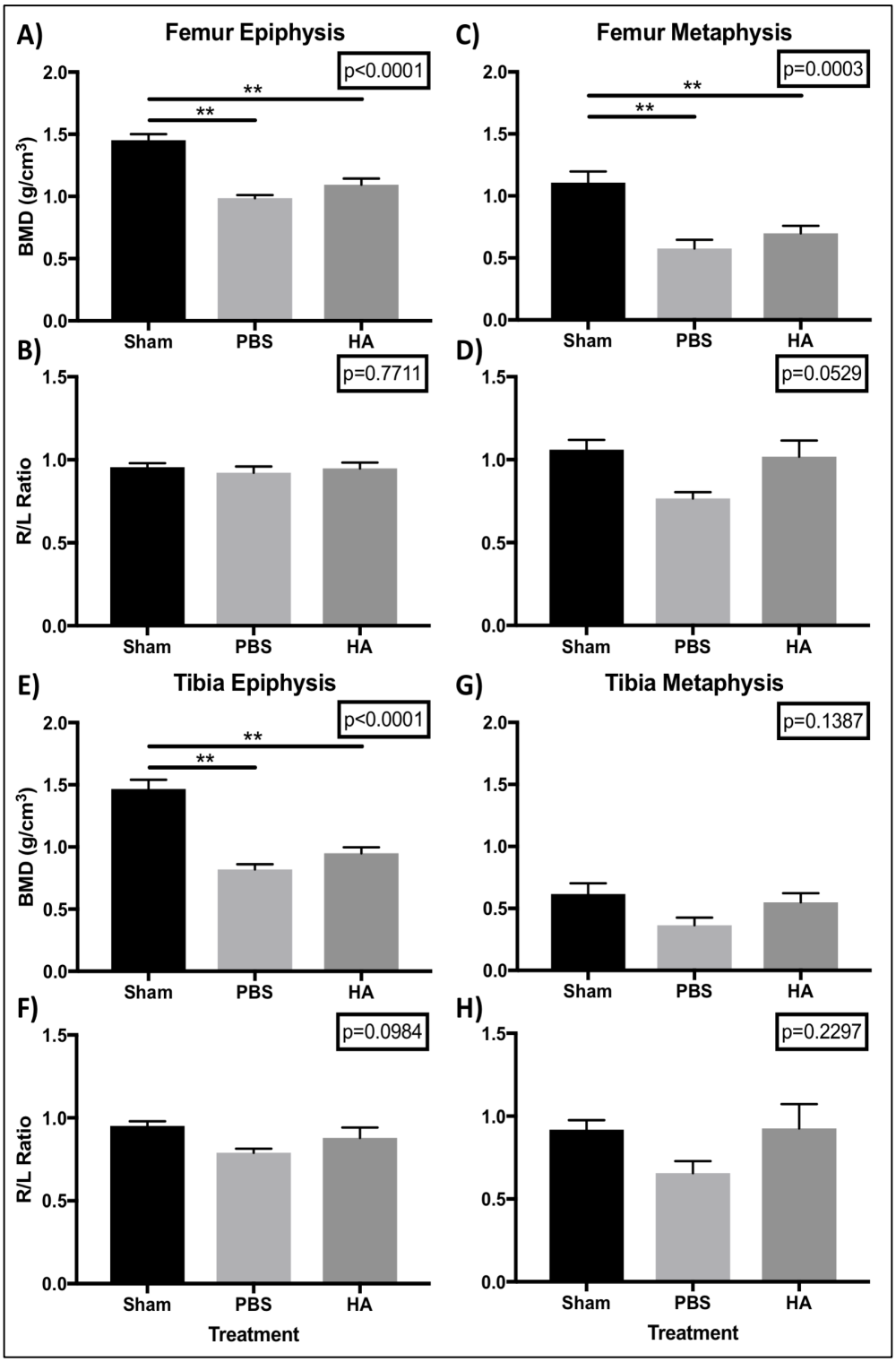

Figure 9: Bone mineral density (BMD) of the femur epiphysis (**A, B**), femur metaphysis (**C, D**), tibia epiphysis (**E, F**) and tibia metaphysis (**G, H**) among Sham, PBS, and HA treatment groups at 9 weeks post-ACLT + pMMT surgery. Absolute (**A, C, E, G**) and normalized (**B, D, F, H**) data are shown. * = $p<0.05$, ** = $p<0.01$.

3.4.2: Trabecular Thickness

A significant effect of treatment on absolute trabecular thickness (Tb.Th) was found for all analyzed bone segments ($p<0.05$ for all). Absolute Tb.Th was significantly higher in the HA group compared to the PBS group at all analyzed bone segments (**Figure 10**). In the femur metaphysis, Tb.Th in the Sham group (0.1150 mm) was significantly higher than that of the PBS group (0.1028 mm, $p<0.05$). Absolute Tb.Th in the of the HA group in the femur epiphysis and tibia metaphysis was also found to be significantly higher than that of the Sham group.

When Tb.Th was normalized to contralateral controls, a significant effect of treatment was only found in the femur metaphysis and tibia epiphysis. Similarly, the only significant differences found among treatment groups were in the femur metaphysis and tibia epiphysis (**Figure 10**). In the femur metaphysis, both Sham (0.9934) and HA (1.006) groups were significantly higher in normalized Tb.Th when compared to that of the PBS group (0.8976, $p<0.05$). In the tibia epiphysis, the Sham group (1.008) was found to have a significantly higher normalized Tb.Th compared to the PBS group (0.8811, $p<0.01$).

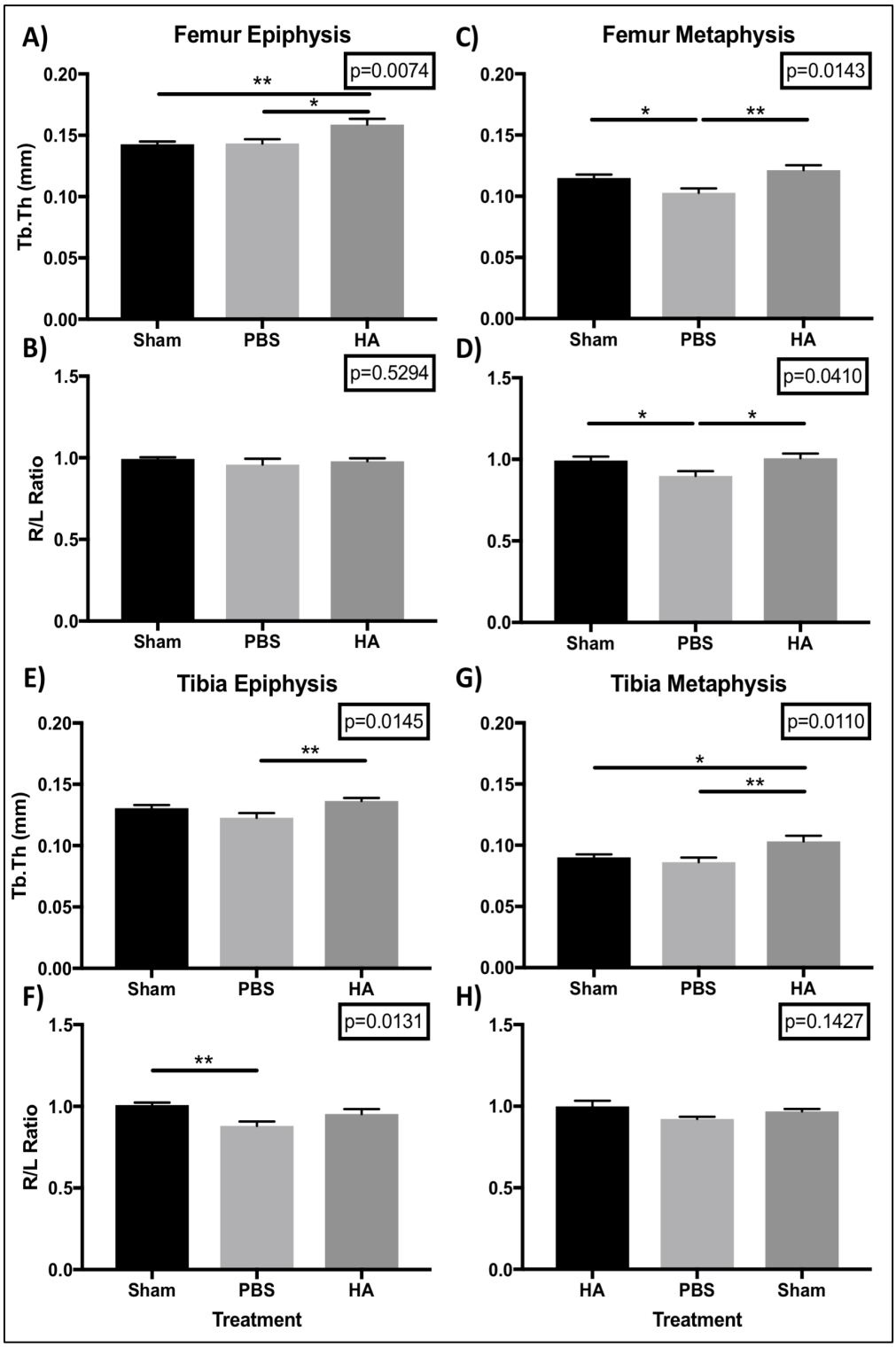

Figure 10: Trabecular thickness (Tb.Th) of the femur epiphysis (**A, B**), femur metaphysis (**C, D**), tibia epiphysis (**E, F**) and tibia metaphysis (**G, H**) among Sham, PBS, and HA treatment groups at 9 weeks post-ACLT + pMMT surgery. Absolute (**A, C, E, G**) and normalized (**B, D, F, H**) data are shown. * = $p<0.05$, ** = $p<0.01$.

3.4.3: Trabecular Number

A significant effect of treatment on absolute trabecular number (Tb.N) was found at all analyzed bone segments (**Figure 11**). Absolute Tb.N in the HA group was found to be significantly lower than that of the Sham group at all analyzed bone segments ($p<0.05$ for femur epiphysis and tibia metaphysis, $p<0.01$ for femur metaphysis and tibia epiphysis). Absolute Tb.N in the PBS group was also significantly lower than that of the Sham group in the femur metaphysis, tibia epiphysis, and tibia metaphysis ($p<0.01$ for all). However, when Tb.N was normalized to contralateral controls, no significant effects of treatment were found at all analyzed bone segments, although a significant decrease in PBS normalized Tb.N was found compared to that of the Sham group in the femur metaphysis and tibia metaphysis ($p<0.05$, **Figure 11**).

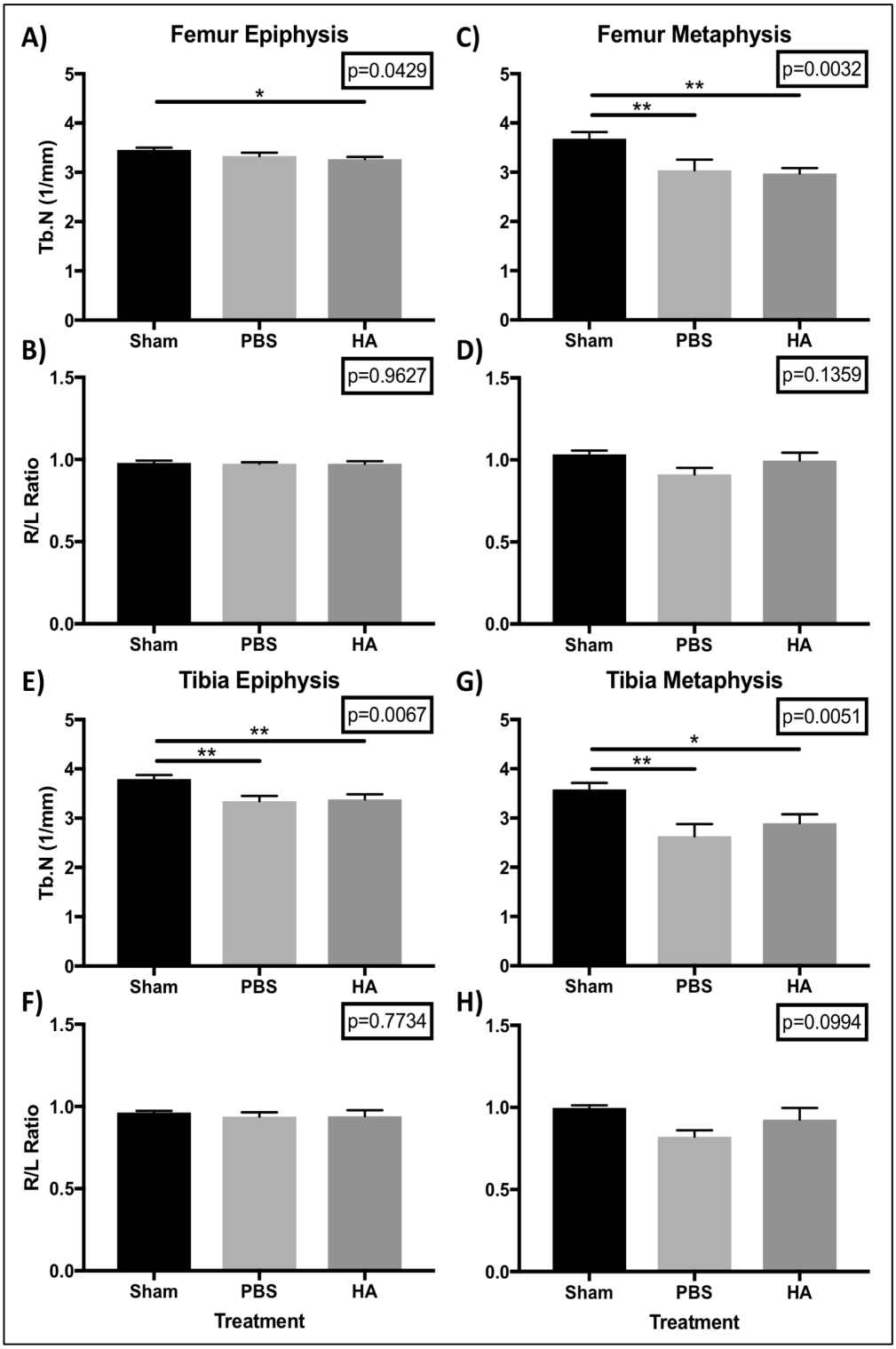

Figure 11: Trabecular number (Tb.N) of the femur epiphysis (**A, B**), femur metaphysis (**C, D**), tibia epiphysis (**E, F**) and tibia metaphysis (**G, H**) among Sham, PBS, and HA treatment groups at 9 weeks post-ACLT + pMMT surgery. Absolute (**A, C, E, G**) and normalized (**B, D, F, H**) data are shown. * = $p<0.05$, ** = $p<0.01$.

3.4.4: Trabecular Separation

No significant effects of treatment on absolute trabecular separation (Tb.Sp) were found at all analyzed bone segments (**Figure 12**). However, a significant increase in absolute Tb.Sp was found in the HA group (0.2856 mm) when compared to that of the Sham group (0.2083 mm) in the femur metaphysis ($p<0.05$). A significant increase in absolute Tb.Sp was also found in the PBS group (0.212 mm) when compared to that of the Sham group (0.1768 mm) in the tibia epiphysis. When Tb.Sp was normalized to contralateral controls, significant effects of treatment and significant differences among treatment groups were not found at any analyzed bone segments (**Figure 12**).

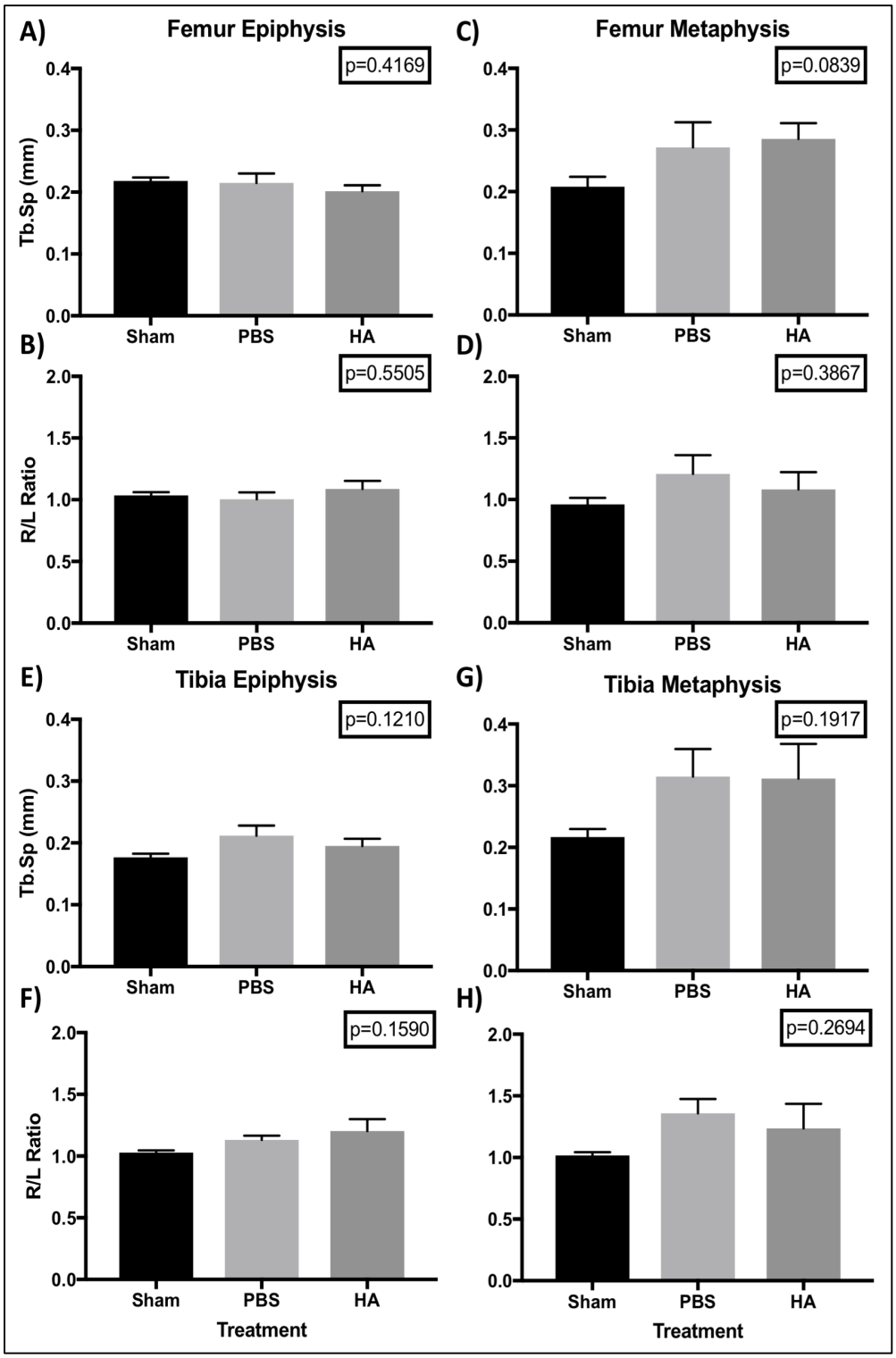

Figure 12: Trabecular separation (Tb.Sp) of the femur epiphysis (**A, B**), femur metaphysis (**C, D**), tibia epiphysis (**E, F**) and tibia metaphysis (**G, H**) among Sham, PBS, and HA treatment groups at 9 weeks post-ACLT + pMMT surgery. Absolute (**A, C, E, G**) and normalized (**B, D, F, H**) data are shown. * = $p<0.05$, ** = $p<0.01$.

3.4.5: Percent Bone Volume

Significant effects of treatment on absolute percent bone volume (BV/TV) were found in the femur metaphysis and tibia epiphysis ($p<0.05$ for both, **Figure 13**). Absolute BV/TV in the PBS group was also found to be significantly lower than that of the Sham group in the femur metaphysis, tibia epiphysis, and tibia metaphysis ($p<0.01$ for femur metaphysis and tibia epiphysis, $p<0.05$ for tibia metaphysis).

When BV/TV was normalized to contralateral controls, significant effects of treatment on BV/TV were maintained in the femur metaphysis ($p=0.0431$), but not the tibia epiphysis ($p=0.0591$). Nevertheless, a significant decrease in normalized BV/TV was found in the PBS group compared to that of the Sham group in both the femur metaphysis and tibia epiphysis ($p<0.05$ for both, **Figure 13**). A significant increase in normalized BV/TV was also found in the HA group (1.011) compared to that of the PBS group (0.8158) in the femur metaphysis ($p<0.05$).

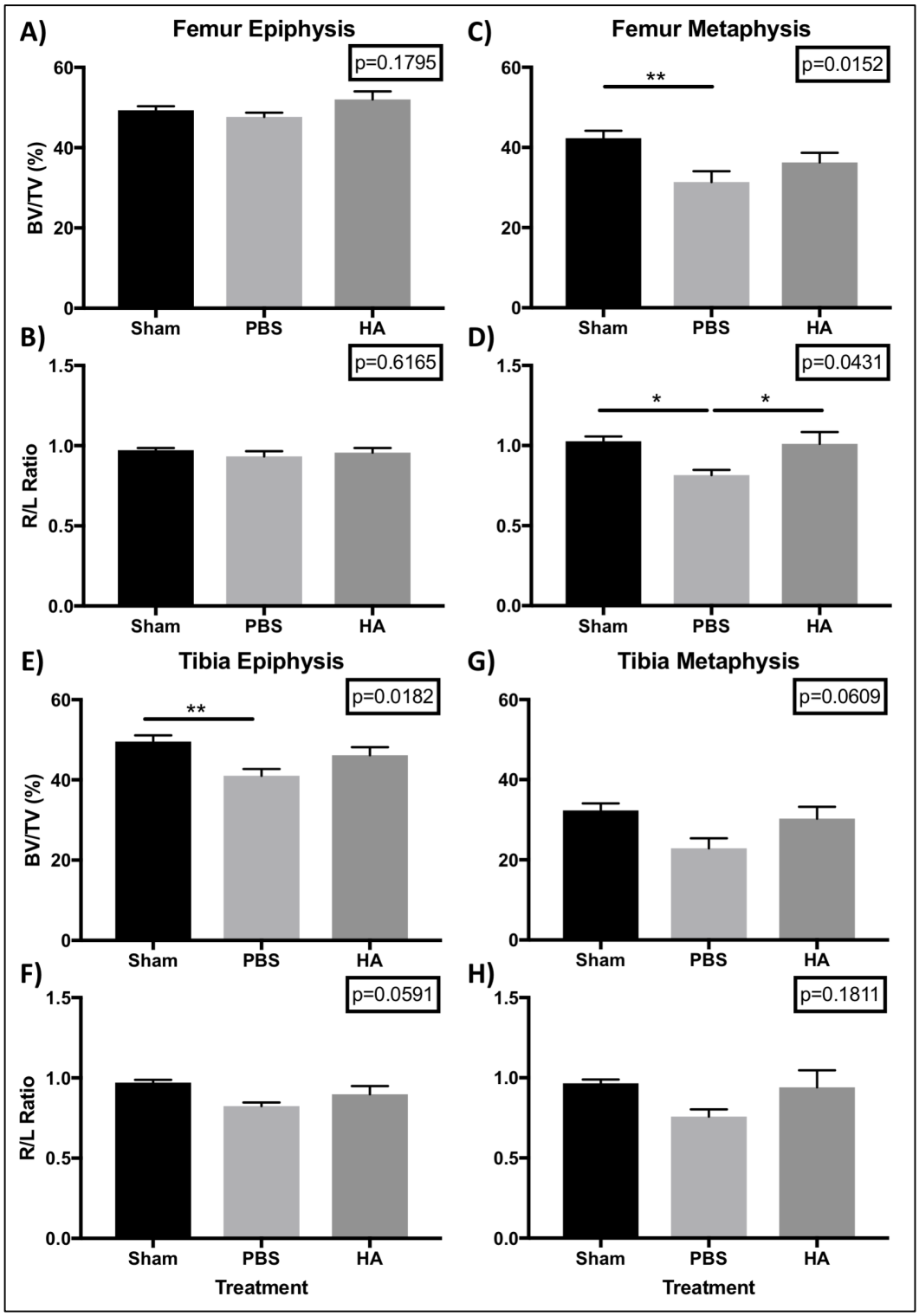

Figure 13: Percent bone volume (BV/TV) of the femur epiphysis (**A, B**), femur metaphysis (**C, D**), tibia epiphysis (**E, F**) and tibia metaphysis (**G, H**) among Sham, PBS, and HA treatment groups at 9 weeks post-ACLT + pMMT surgery. Absolute (**A, C, E, G**) and normalized (**B, D, F, H**) data are shown. * = $p<0.05$, ** = $p<0.01$.

3.4.6: Bone Surface Density

A significant effect of treatment on absolute bone surface density (BS/TV) was found only at the tibia metaphysis ($p=0.0428$). A significant decrease in BS/TV in the tibia metaphysis was found in the PBS group (10.23 mm^{-1}) when compared to that of the Sham group (12.68 mm^{-1}). However, when BS/TV was normalized to contralateral controls, significant effects of treatment and significant differences among treatment groups were not found at any analyzed bone segments (**Figure 14**).

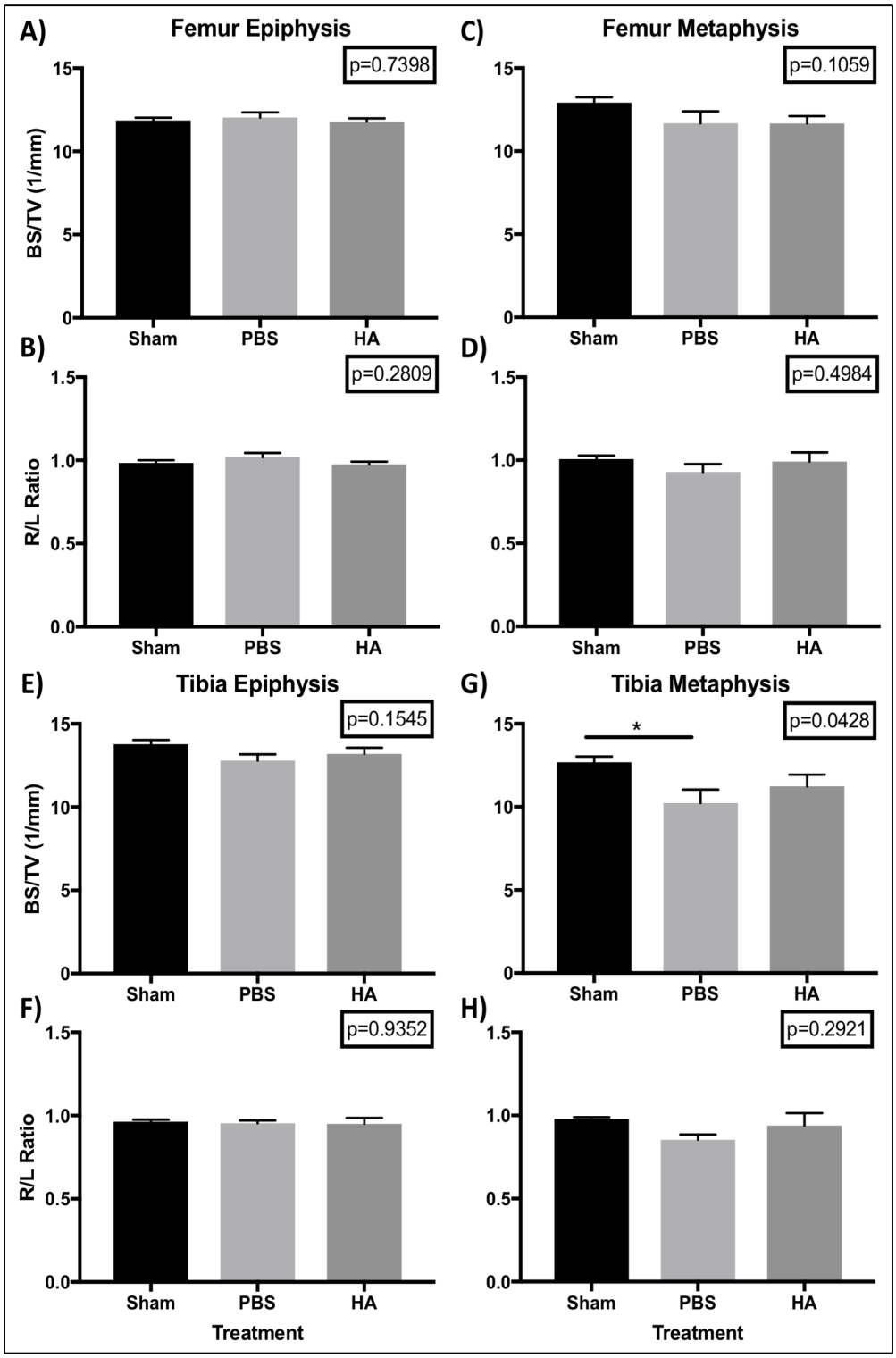

Figure 14: Bone surface density (BS/TV) of the femur epiphysis (**A, B**), femur metaphysis (**C, D**), tibia epiphysis (**E, F**) and tibia metaphysis (**G, H**) among Sham, PBS, and HA treatment groups at 9 weeks post-ACLT + pMMT surgery. Absolute (**A, C, E, G**) and normalized (**B, D, F, H**) data are shown. * = $p<0.05$, ** = $p<0.01$.

4. DISCUSSION

In this study, ACLT + pMMT surgeries were performed on rats to investigate behavioral, cartilage, and bone changes in early PTOA. Additionally, an intra-articular injection of hyaluronic acid was administered at 1 week post-surgery to investigate its attenuating effect on early PTOA changes in cartilage and bone. The results indicate that ACLT + pMMT surgery resulted in a temporary contralateral preference in static weight bearing, minor degeneration of the articular cartilage, and generally decreased bone quality. However, among the parameters analyzed, trabecular thickness of the μCT analyses was the most sensitive parameter for characterizing PTOA changes in the ACLT + pMMT model among all measured parameters. Treatment with HA was also found to attenuate the progression of PTOA changes in articular cartilage and bone morphology.

The animals used in this study were 9-10 weeks old at the time of the surgeries, which is beyond the 8-week threshold for rat adulthood (47). Although all animals were skeletally mature at 0W, differences in body weight among treatment groups were observed. Since animals of the same strain were expected from the vendor, similar weights among the animals were expected as well. However, these differences could be due to the 1-week difference in age among some animals in the study. While most animals may have already reached the plateau of the growth curve, it is possible that rats that were 1 week younger were still at the late stages of exponential growth (48). At the end of the study, no significant differences in body weight were observed among groups. Furthermore, the age of the rats used in this study resembles that of young adult humans (47). It would be

important, however, to investigate the effects of age on responses to ACLT + pMMT in a future study.

The ACLT + pMMT combination surgery for knee OA induction was utilized in this study because preliminary studies performed in our lab found that ACLT + pMMT showed a milder, but detectable degeneration progression of OA cartilage and bone changes compared to ACLT or MMT alone. Furthermore, it was expected to observe degeneration of the articular cartilage and bone by performing minimally invasive ACLT + pMMT surgeries to reproduce PTOA in a rat model similar to that in humans due to ACL tear and meniscus damage.

The changes observed in this study reflect early PTOA changes because the terminal time point in this study was 9 weeks after the ACLT + pMMT surgery. PTOA is a disease that develops over a long period of time, taking anywhere from 6 months to decades to develop (49-51). For example, it has been reported that it took, on average, 22 years after sustaining a knee injury for symptomatic OA be diagnosed in a young cohort of medical students who had experienced knee injuries (mean age at time of injury: 22 years) (52). Therefore, the scope of this study is limited to early PTOA changes and not moderate- or end-stage PTOA.

The changes in behavior due to ACLT + pMMT were tested using Von Frey nociception and incapacitance tests. In the Von Frey nociception test, significant differences were only observed at 1 week after the surgeries. At 0W, all animals showed negative responses when hind paws were stimulated with Von Frey filaments, with 50% paw withdrawal threshold at 15 g for all groups (**Figure 5**). At 1W the 50% paw withdrawal threshold of the Sham group decreased along with that of the PBS and Sham groups. At

1W, the HA group was found to be significantly lower than that of the Sham and PBS groups. The 1W Von Frey measurements were taken before the treatment injections were administered at 1W; therefore, the observed differences are not due to any injection treatment and must be due to the surgery. Furthermore, no significant differences were observed at any other time points, and all groups had generally returned to normal by 4W. This suggests that the decreases in 50% paw withdrawal threshold at 1W are mainly due to pain from the skin incision, joint capsule incision, and patellar dislocation during the surgical procedures and not the ACLT + pMMT procedures.

In contrast, the incapacitance tests showed that HLWD of the Sham group was significantly higher than both HA and PBS groups at 1W, 2W, and 3W time points. Unlike what was observed in the Von Frey nociception test, HLWD of the Sham group remained around 50% throughout the duration of the study. In contrast, both HA and PBS groups dropped to approximately 40% HLWD at 1W. This suggests that the observed changes in static weight bearing are due to ACLT + pMMT and not to any surgical access procedures performed. At 4W, 3 weeks after the injection treatments, both HA and PBS groups had returned to normal HLWD. The fact that there were no significant differences in HLWD between PBS and HA groups at any time point suggests that a mere 4 weeks of recovery after ACLT + pMMT surgery is sufficient to regain normal HLWD. Therefore, the injection treatments had little to no effect on restoring static weight bearing due to ACLT + pMMT surgery.

Although histological analyses of the PBS group tended to yield higher OARSI scores compared to that of the HA group, there were no significant differences between the two groups (**Figure 7B**). Most histological changes observed in the MTP due to ACLT +

pMMT surgery in this study were minor. However, there have been publications reporting much more severe histological changes due to surgical induction of knee OA, some even at time points earlier than reported in our study (33, 34, 53-55). For example, Gerwin et al. reported cartilage lesions spanning the entire depth of the knee cartilage at 3 weeks following full MMT surgery, which translates to an OARSI score of 10 to 12 (33). However, in the present study and in our pilot studies, such severe cartilage lesions were not observed after ACLT only, MMT only, or ACLT + pMMT surgical procedures. The highest OARSI score observed from a single sample in this 9-week study was a 9 from the PBS group, although the average score of the group was 3.6 (**Figure 7B**). It is possible that the discrepancy in cartilage degeneration is due to inconsistencies in surgical invasiveness among labs. During the surgical procedures performed in this study, incisions were made as minimally invasive as possible as to avoid bleeding and prevent blood from entering the joint. This is important because damage to articular cartilage due to the mere presentation of blood in joints (hemarthrosis) has been reported (56-61). In this study, minimally invasive surgical techniques were utilized to investigate OA changes without the confounding factor of hemarthrosis such that changes due only to the ACLT + pMMT surgery itself could be observed. Because there were no significant differences in histological changes found between the injection treatment groups in this 9-week study, histological analyses are not ideal for identifying early PTOA changes in the knee.

In the μCT analyses, bone quality was generally higher in the Sham and HA groups compared to the PBS group, and no significant differences were found between the Sham and HA groups (**Table 4**). Most of the significant differences found between treatment groups were present in the femur metaphysis and the tibia epiphysis. Although significant

differences in absolute values between groups were observed at all analyzed bone segments for some bone parameters, these significant differences remained only in the femur metaphysis and tibia epiphysis when the data were normalized to the left contralateral control knees (**Figure 10**). This suggests that the femur metaphysis and tibia epiphysis are particularly sensitive to early PTOA changes in bone due to ACLT + pMMT surgery.

Table 4: Summary of μCT results. Differences observed normalized values of the femur metaphysis are shown. Directions within each column are relative to the first group mentioned. ↑ = Significant increase, ↔ = No significant differences.

Bone Parameter	Sham / PBS	Sham / HA	HA / PBS
BMD	↑	↔	↑
Tb.Th	↑	↔	↑
Tb.N	↑	↔	↔
Tb.Sp	↔	↔	↔
BV/TV	↑	↔	↑
BS/TV	↔	↔	↔

Furthermore, among the bone parameters measured, only BMD, Tb.Th, and BV/TV maintained significant effects of treatment on the measured parameter after the data was normalized to those of contralateral controls. These results are remarkable because a previous 10-week study using MMT in rats reported no significant changes in BMD and Tb.Th but significant decreases in BV/TV and Tb.N, and significant increases in Tb.Sp (34). These inconsistences in findings support the idea that surgical invasiveness needs to be standardized among labs so that bone changes due to surgical induction of OA are consistent. Nevertheless, the bone segment that consistently maintains significant effects of treatment after normalization of both BMD and BV/TV is the femur metaphysis. However, in Tb.Th, significant effects of treatment after normalization is maintained in both the femur metaphysis and tibia epiphysis (**Figure 10**). Therefore, based on these

results, it can be concluded that the femur metaphysis is the bone segment most sensitive to ACLT + pMMT surgery, and that among the bone parameters analyzed in this study, Tb.Th is the most sensitive parameter in detecting PTOA changes.

When comparing bone parameter measurements between the injection treatment groups, the HA group was found to have a higher BMD, Tb.Th, and BV/TV compared to those of the PBS group (**Table 4**). Additionally, the Sham group showed significantly higher normalized BMD, Tb.Th, Tb.N, and BV/TV compared to the PBS group, and there were no significant differences between Sham and HA groups for any of the analyzed bone parameters. ACLT+ pMMT surgery was expected to cause a decrease in bone quality, as evidenced by the PBS group. However, some of the bone parameters measured in the HA injection group were closer to those of the Sham group. This suggests that injection of HA at one week after ACLT + pMMT surgery was successful in attenuating some early PTOA changes in bone quality. These results add to the many reports on the efficacy of HA injection in animal models (17, 18, 21-28), although the use of HA for clinical treatment of knee osteoarthritis is still not recommended (29). In the future, it may be useful to investigate the effects of administrating HA injections at different time points on PTOA changes.

The bone changes observed in this study can be attributed to disuse of the operated hind limb. The incapacitance tests revealed significant differences in static weight bearing in the PBS and HA groups at 1W, 2W, and 3W time points when compared to the Sham group, which maintained roughly 50% HLWD throughout the duration of the study (**Figure 6**). From 4W onward, all groups maintained approximately 50% HLWD until the end of the study. The recovery of HLWD after 4W suggests that ACL injury itself and not

cartilage degeneration was the cause of the significant differences observed at earlier time points, because true cartilage degeneration would have resulted in a progression of lower HLWD. These results show that after ACLT + pMMT surgery there was a preference for bearing weight on the left, contralateral knee. This means that less weight was applied to the right hind limb than it was normally accustomed to experiencing at the 0W time point before the surgical procedures. According to Wolff's law, a bone will undergo morphological changes to adapt to loads that are applied to it (62, 63). Similarly, a bone will undergo morphological changes to adapt to loads removed from it. This may explain why BMD, Tb.Th, Tb.N, and BV/TV were decreased in the femur and tibia in the PBS group at the end of the study. This also suggests that 3 weeks of uneven static hind limb weight bearing after ACLT + pMMT could affect bone measurements 6 weeks later, although more bone analyses at different time points are required to support this conclusion.

It is important to note that Wistar rats were used in this study. Although many knee OA studies report using Sprague-Dawley rats, Lewis rats are preferred for MMT and ACLT + pMMT models because Lewis rats tend to exhibit uniform cartilage degeneration across the MTP, whereas Sprague-Dawley rats tend to exhibit greater cartilage degeneration in the center of the MTP (33). However, Wistar rats were selected for this study based on other reports using Wistar rats to study pain and related changes in behavior due to induced knee OA (43, 54, 64, 65). Although significant changes in the MTP due to ACLT + pMMT were not found in this study using Wistar rats, significant changes in static weight bearing and bone morphology were still found. Given that this 9-week study resulted in early PTOA changes, it is possible that significant changes in the knee articular cartilage could develop if PTOA was allowed a longer time to progress.

In this study, ACLT + pMMT surgery resulted in minor changes in the articular cartilage. Because clinical OA is typically marked with the wearing a way of articular cartilage, exposing the subchondral bone (3, 10), it may be useful to introduce a transection of the medial collateral ligament (MCL) in addition to ACLT + pMMT to cause more severe cartilage damage (66, 67). However, caution must be taken to not cause severe cartilage damage to the point of no regeneration potential, especially for investigating therapeutic interventions for knee OA. Reproducing end-stage OA in animal models holds little value for potential therapeutic interventions because clinical end-stage OA typically results in total knee arthroplasty. Therefore, an ideal animal model used for investigating therapeutic interventions for knee OA in the future should develop, at most, moderate knee OA cartilage degeneration to preserve the regenerative potential of the knee cartilage and consistently use minimally invasive surgical techniques to avoid unwanted joint damage during surgery (33).

Additionally, intra-articular HA injections administered at 1 week after ACLT + pMMT surgeries were found to attenuate cartilage and bone changes. Histological scores of the HA group tended to be lower than that of the PBS group, suggesting that cartilage degeneration was attenuated. Bone μCT measures in the HA group were closer to that of the Sham group and were significantly greater than that of the PBS group, suggesting that HA injections also attenuate OA bone changes. It is important to note that HA injections are administered to prevent PTOA disease progression and do not aim to restore cartilage and bone changes that may have already occurred because of the disease. In this study, PTOA was allowed to progress for 8 weeks after ACLT + pMMT surgery, allowing for early-PTOA changes to occur in the cartilage and bone. Therefore, it would be important

to investigate the effects of HA injection given a longer time course for PTOA to progress in a future study.

In conclusion, this study found that bone analyses, specifically trabecular thickness measurement, can be used as outcome measures of knee OA treatment. Additionally, surgical induction of knee OA by ACLT + pMMT in Wistar rats caused early PTOA changes, although intra-articular HA injections were successful in attenuating these changes, as suggested by static weight bearing tests and confirmed by μCT bone analyses.

I would like to acknowledge Kenji Kato, Shingo Miyazaki, and Junichi Yamada of the Skeletal Translational Research Laboratory in the Department of Orthopaedic Surgery at UCSD as co-authors for their indispensable help on the work presented in this thesis. The presented study may be prepared for publication in the future. Kevin Cheng was the primary investigator and author of this study.

5. REFERENCES

1. Zhang Y, Jordan JM. Epidemiology of osteoarthritis. Clin Geriatr Med. 2010;26(3):355-69. doi: 10.1016/j.cger.2010.03.001. PubMed PMID: 20699159; PMCID: PMC2920533.

2. Helmick CG. The Burden of Musculoskeletal Diseases in the United States: Prevalence of Arthritic Conditions; 2014 [cited 2017 5 June]. Available from: http://www.boneandjointburden.org/2014-report/ivb0/prevalence-arthritic-conditions.

3. Heidari B. Knee osteoarthritis prevalence, risk factors, pathogenesis and features: Part I. Caspian J Intern Med. 2011;2(2):205-12. PubMed PMID: 24024017; PMCID: PMC3766936.

4. Johnson VL, Hunter DJ. The epidemiology of osteoarthritis. Best Pract Res Clin Rheumatol. 2014;28(1):5-15. doi: 10.1016/j.berh.2014.01.004. PubMed PMID: 24792942.

5. Anderson DD, Chubinskaya S, Guilak F, Martin JA, Oegema TR, Olson SA, Buckwalter JA. Post-traumatic osteoarthritis: improved understanding and opportunities for early intervention. J Orthop Res. 2011;29(6):802-9. doi: 10.1002/jor.21359. PubMed PMID: 21520254; PMCID: PMC3082940.

6. Balazs EA. The Physical Properties of Synovial Fluid and the Special Role of Hyaluronic Acid. Disorders of the Knee. 1974:63-75.

7. Tamer TM. Hyaluronan and synovial joint: function, distribution and healing. Interdiscip Toxicol. 2013;6(3):111-25. doi: 10.2478/intox-2013-0019. PubMed PMID: 24678248; PMCID: PMC3967437.

8. French HP, Smart KM, Doyle F. Prevalence of neuropathic pain in knee or hip osteoarthritis: A systematic review and meta-analysis. Semin Arthritis Rheum. 2017. doi: 10.1016/j.semarthrit.2017.02.008. PubMed PMID: 28320529.

9. Samson DJ, Grant MD, Ratko TA, Bonnell CJ, Ziegler KM, Aronson N. Treatment of primary and secondary osteoarthritis of the knee. Evid Rep Technol Assess (Full Rep). 2007(157):1-157. PubMed PMID: 18088162; PMCID: PMC4781439.

10. Wieland HA, Michaelis M, Kirschbaum BJ, Rudolphi KA. Osteoarthritis - an untreatable disease? Nat Rev Drug Discov. 2005;4(4):331-44. doi: 10.1038/nrd1693. PubMed PMID: 15803196.

11. Egloff C, Hugle T, Valderrabano V. Biomechanics and pathomechanisms of osteoarthritis. Swiss Med Wkly. 2012;142:w13583. doi: 10.4414/smw.2012.13583. PubMed PMID: 22815119.

12. Lohmander LS, Lark MW, Dahlberg L, Walakovits LA, Roos H. Cartilage matrix metabolism in osteoarthritis: markers in synovial fluid, serum, and urine. Clin Biochem. 1992;25(3):167-74. PubMed PMID: 1633631.

13. Buckland-Wright C. Subchondral bone changes in hand and knee osteoarthritis detected by radiography. Osteoarthritis Cartilage. 2004;12 Suppl A:S10-9. PubMed PMID: 14698636.

14. Poulet B, de Souza R, Kent AV, Saxon L, Barker O, Wilson A, Chang YM, Cake M, Pitsillides AA. Intermittent applied mechanical loading induces subchondral bone thickening that may be intensified locally by contiguous articular cartilage lesions. Osteoarthritis Cartilage. 2015;23(6):940-8. doi: 10.1016/j.joca.2015.01.012. PubMed PMID: 25655679; PMCID: PMC4459965.

15. Goldring MB, Otero M. Inflammation in osteoarthritis. Curr Opin Rheumatol. 2011;23(5):471-8. doi: 10.1097/BOR.0b013e328349c2b1. PubMed PMID: 21788902; PMCID: PMC3937875.

16. Goldring MB, Otero M, Plumb DA, Dragomir C, Favero M, El Hachem K, Hashimoto K, Roach HI, Olivotto E, Borzi RM, Marcu KB. Roles of inflammatory and anabolic cytokines in cartilage metabolism: signals and multiple effectors converge upon MMP-13 regulation in osteoarthritis. Eur Cell Mater. 2011;21:202-20. PubMed PMID: 21351054; PMCID: PMC3937960.

17. Goldberg VM, Buckwalter JA. Hyaluronans in the treatment of osteoarthritis of the knee: evidence for disease-modifying activity. Osteoarthritis Cartilage. 2005;13(3):216-24. doi: 10.1016/j.joca.2004.11.010. PubMed PMID: 15727888.

18. Migliore A, Procopio S. Effectiveness and utility of hyaluronic acid in osteoarthritis. Clin Cases Miner Bone Metab. 2015;12(1):31-3. doi: 10.11138/ccmbm/2015.12.1.031. PubMed PMID: 26136793; PMCID: PMC4469223.

19. Zhang W, Moskowitz RW, Nuki G, Abramson S, Altman RD, Arden N, Bierma-Zeinstra S, Brandt KD, Croft P, Doherty M, Dougados M, Hochberg M, Hunter DJ, Kwoh K, Lohmander LS, Tugwell P. OARSI recommendations for the management of hip and knee osteoarthritis, part I: critical appraisal of existing treatment guidelines and systematic review of current research evidence. Osteoarthritis Cartilage. 2007;15(9):981-1000. doi: 10.1016/j.joca.2007.06.014. PubMed PMID: 17719803.

20. Jordan KM, Arden NK, Doherty M, Bannwarth B, Bijlsma JW, Dieppe P, Gunther K, Hauselmann H, Herrero-Beaumont G, Kaklamanis P, Lohmander S, Leeb B, Lequesne M, Mazieres B, Martin-Mola E, Pavelka K, Pendleton A, Punzi L, Serni U, Swoboda B, Verbruggen G, Zimmerman-Gorska I, Dougados M, Standing Committee for International Clinical Studies Including Therapeutic Trials E. EULAR Recommendations 2003: an evidence based approach to the management of knee osteoarthritis: Report of a Task Force of the Standing Committee for International Clinical Studies Including Therapeutic Trials (ESCISIT). Ann Rheum Dis. 2003;62(12):1145-55. PubMed PMID: 14644851; PMCID: PMC1754382.

21. Aggarwal A, Sempowski IP. Hyaluronic acid injections for knee osteoarthritis. Systematic review of the literature. Can Fam Physician. 2004;50:249-56. PubMed PMID: 15000336; PMCID: PMC2214549.

22. Dernek B, Duymus TM, Koseoglu PK, Aydin T, Kesiktas FN, Aksoy C, Mutlu S. Efficacy of single-dose hyaluronic acid products with two different structures in patients with early-stage knee osteoarthritis. J Phys Ther Sci. 2016;28(11):3036-40. doi: 10.1589/jpts.28.3036. PubMed PMID: 27942115; PMCID: PMC5140795.

23. Levillain A, Magoariec H, Boulocher C, Decambron A, Viateau V, Hoc T. Effects of a viscosupplementation therapy on rabbit menisci in an anterior cruciate ligament transection model of osteoarthritis. J Biomech. 2017. doi: 10.1016/j.jbiomech.2017.04.034. PubMed PMID: 28554494.

24. Lu HT, Sheu MT, Lin YF, Lan J, Chin YP, Hsieh MS, Cheng CW, Chen CH. Injectable hyaluronic-acid-doxycycline hydrogel therapy in experimental rabbit osteoarthritis. BMC Vet Res. 2013;9:68. doi: 10.1186/1746-6148-9-68. PubMed PMID: 23574696; PMCID: PMC3637605.

25. Ong KL, Anderson AF, Niazi F, Fierlinger AL, Kurtz SM, Altman RD. Hyaluronic Acid Injections in Medicare Knee Osteoarthritis Patients Are Associated With Longer Time to Knee Arthroplasty. J Arthroplasty. 2016;31(8):1667-73. doi: 10.1016/j.arth.2016.01.038. PubMed PMID: 26895820.

26. Shewale AR, Fischbach LA, Hammond DA, Martin BC. Letter to the Editor on 'Hyaluronic Acid Injections in Medicare Knee Osteoarthritis Patients Are Associated With Longer Time to Knee Arthroplasty'. J Arthroplasty. 2017;32(2):696-7. doi: 10.1016/j.arth.2016.08.042. PubMed PMID: 27780624.

27. Vaishya R, Pandit R, Agarwal AK, Vijay V. Intra-articular hyaluronic acid is superior to steroids in knee osteoarthritis: A comparative, randomized study. J Clin Orthop Trauma. 2017;8(1):85-8. doi: 10.1016/j.jcot.2016.09.008. PubMed PMID: 28360505; PMCID: PMC5359523.

28. Yanagisawa K, Muneta T, Ozeki N, Nakagawa Y, Udo M, Saito R, Koga H, Tsuji K, Sekiya I. Weekly injections of Hylan G-F 20 delay cartilage degeneration in partial meniscectomized rat knees. BMC Musculoskelet Disord. 2016;17:188. doi: 10.1186/s12891-016-1051-6. PubMed PMID: 27118194; PMCID: PMC4847373.

29. Treatment of Osteoarthritis of the Knee - 2nd Edition. American Academy of Orthopaedic Surgeons, 2013.

30. Gregory MH, Capito N, Kuroki K, Stoker AM, Cook JL, Sherman SL. A review of translational animal models for knee osteoarthritis. Arthritis. 2012;2012:764621. doi: 10.1155/2012/764621. PubMed PMID: 23326663; PMCID: PMC3541554.

31. Suokas AK, Sagar DR, Mapp PI, Chapman V, Walsh DA. Design, study quality and evidence of analgesic efficacy in studies of drugs in models of OA pain: a systematic review and a meta-analysis. Osteoarthritis Cartilage. 2014;22(9):1207-23. doi: 10.1016/j.joca.2014.06.015. PubMed PMID: 25008207.

32. Teeple E, Jay GD, Elsaid KA, Fleming BC. Animal models of osteoarthritis: challenges of model selection and analysis. AAPS J. 2013;15(2):438-46. doi: 10.1208/s12248-013-9454-x. PubMed PMID: 23329424; PMCID: PMC3675748.

33. Gerwin N, Bendele AM, Glasson S, Carlson CS. The OARSI histopathology initiative - recommendations for histological assessments of osteoarthritis in the rat. Osteoarthritis Cartilage. 2010;18 Suppl 3:S24-34. doi: 10.1016/j.joca.2010.05.030. PubMed PMID: 20864021.

34. Bagi CM, Zakur DE, Berryman E, Andresen CJ, Wilkie D. Correlation between muCT imaging, histology and functional capacity of the osteoarthritic knee in the rat model

of osteoarthritis. J Transl Med. 2015;13:276. doi: 10.1186/s12967-015-0641-7. PubMed PMID: 26303725; PMCID: PMC4549091.

35. Migliore A, Giovannangeli F, Granata M, Lagana B. Hylan g-f 20: review of its safety and efficacy in the management of joint pain in osteoarthritis. Clin Med Insights Arthritis Musculoskelet Disord. 2010;3:55-68. PubMed PMID: 21151854; PMCID: PMC2998981.

36. Zhao H, Liu H, Liang X, Li Y, Wang J, Liu C. Hylan G-F 20 Versus Low Molecular Weight Hyaluronic Acids for Knee Osteoarthritis: A Meta-Analysis. BioDrugs. 2016;30(5):387-96. doi: 10.1007/s40259-016-0186-1. PubMed PMID: 27435213.

37. Bonin RP, Bories C, De Koninck Y. A simplified up-down method (SUDO) for measuring mechanical nociception in rodents using von Frey filaments. Mol Pain. 2014;10:26. doi: 10.1186/1744-8069-10-26. PubMed PMID: 24739328; PMCID: PMC4020614.

38. Pitcher GM, Ritchie J, Henry JL. Paw withdrawal threshold in the von Frey hair test is influenced by the surface on which the rat stands. J Neurosci Methods. 1999;87(2):185-93. PubMed PMID: 11230815.

39. Neugebauer V, Han JS, Adwanikar H, Fu Y, Ji G. Techniques for assessing knee joint pain in arthritis. Mol Pain. 2007;3:8. doi: 10.1186/1744-8069-3-8. PubMed PMID: 17391515; PMCID: PMC1851005.

40. Piel MJ, Kroin JS, Im HJ. Assessment of knee joint pain in experimental rodent models of osteoarthritis. Methods Mol Biol. 2015;1226:175-81. doi: 10.1007/978-1-4939-1619-1_13. PubMed PMID: 25331050; PMCID: PMC4511105.

41. Chaplan SR, Bach FW, Pogrel JW, Chung JM, Yaksh TL. Quantitative assessment of tactile allodynia in the rat paw. J Neurosci Methods. 1994;53(1):55-63. PubMed PMID: 7990513.

42. Dixon WJ. Efficient analysis of experimental observations. Annu Rev Pharmacol Toxicol. 1980;20:441-62. doi: 10.1146/annurev.pa.20.040180.002301. PubMed PMID: 7387124.

43. Angeby Moller K, Svard H, Suominen A, Immonen J, Holappa J, Stenfors C. Gait analysis and weight bearing in pre-clinical joint pain research. J Neurosci Methods. 2017. doi: 10.1016/j.jneumeth.2017.04.011. PubMed PMID: 28445709.

44. Wu YT, Wu PT, Jou IM. Peritendinous elastase treatment induces tendon degeneration in rats: A potential model of tendinopathy in vivo. J Orthop Res. 2016;34(3):471-7. doi: 10.1002/jor.23030. PubMed PMID: 26291184.

45. Bouxsein ML, Boyd SK, Christiansen BA, Guldberg RE, Jepsen KJ, Muller R. Guidelines for assessment of bone microstructure in rodents using micro-computed tomography. J Bone Miner Res. 2010;25(7):1468-86. doi: 10.1002/jbmr.141. PubMed PMID: 20533309.

46. Pritzker KP, Gay S, Jimenez SA, Ostergaard K, Pelletier JP, Revell PA, Salter D, van den Berg WB. Osteoarthritis cartilage histopathology: grading and staging. Osteoarthritis Cartilage. 2006;14(1):13-29. doi: 10.1016/j.joca.2005.07.014. PubMed PMID: 16242352.

47. Sengupta P. The Laboratory Rat: Relating Its Age With Human's. Int J Prev Med. 2013;4(6):624-30. PubMed PMID: 23930179; PMCID: PMC3733029.

48. Aguilar C, Friedli C, Canas R. The Growth Curve of Animals. Agr Syst. 1983;10(3):133-47. doi: Doi 10.1016/0308-521x(83)90066-5. PubMed PMID: WOS:A1983QQ70500001.

49. Heidari B. Knee osteoarthritis diagnosis, treatment and associated factors of progression: part II. Caspian J Intern Med. 2011;2(3):249-55. PubMed PMID: 24049581; PMCID: PMC3770501.

50. Lieberthal J, Sambamurthy N, Scanzello CR. Inflammation in joint injury and post-traumatic osteoarthritis. Osteoarthritis Cartilage. 2015;23(11):1825-34. doi: 10.1016/j.joca.2015.08.015. PubMed PMID: 26521728; PMCID: PMC4630675.

51. Little CB, Hunter DJ. Post-traumatic osteoarthritis: from mouse models to clinical trials. Nat Rev Rheumatol. 2013;9(8):485-97. doi: 10.1038/nrrheum.2013.72. PubMed PMID: 23689231.

52. Gelber AC, Hochberg MC, Mead LA, Wang NY, Wigley FM, Klag MJ. Joint injury in young adults and risk for subsequent knee and hip osteoarthritis. Ann Intern Med. 2000;133(5):321-8. PubMed PMID: 10979876.

53. Appleton CT, McErlain DD, Pitelka V, Schwartz N, Bernier SM, Henry JL, Holdsworth DW, Beier F. Forced mobilization accelerates pathogenesis: characterization of a preclinical surgical model of osteoarthritis. Arthritis Res Ther. 2007;9(1):R13. doi: 10.1186/ar2120. PubMed PMID: 17284317; PMCID: PMC1860072.

54. Iijima H, Aoyama T, Ito A, Tajino J, Nagai M, Zhang X, Yamaguchi S, Akiyama H, Kuroki H. Destabilization of the medial meniscus leads to subchondral bone defects and site-specific cartilage degeneration in an experimental rat model. Osteoarthritis Cartilage. 2014;22(7):1036-43. doi: 10.1016/j.joca.2014.05.009. PubMed PMID: 24857975.

55. Karahan S, Kincaid SA, Kammermann JR, Wright JC. Evaluation of the rat stifle joint after transection of the cranial cruciate ligament and partial medial meniscectomy. Comp Med. 2001;51(6):504-12. PubMed PMID: 11924812.

56. Jansen NW, Roosendaal G, Hooiveld MJ, Bijlsma JW, van Roon JA, Theobald M, Lafeber FP. Interleukin-10 protects against blood-induced joint damage. Br J Haematol. 2008;142(6):953-61. doi: 10.1111/j.1365-2141.2008.07278.x. PubMed PMID: 18637801.

57. Niibayashi H, Shimizu K, Suzuki K, Yamamoto S, Yasuda T, Yamamuro T. Proteoglycan degradation in hemarthrosis. Intraarticular, autologous blood injection in rat knees. Acta Orthop Scand. 1995;66(1):73-9. PubMed PMID: 7863774.

58. Roosendaal G, TeKoppele JM, Vianen ME, van den Berg HM, Lafeber FP, Bijlsma JW. Blood-induced joint damage: a canine in vivo study. Arthritis Rheum. 1999;42(5):1033-9. doi: 10.1002/1529-0131(199905)42:5<1033::AID-ANR24>3.0.CO;2-#. PubMed PMID: 10323461.

59. Sen D, Chapla A, Walter N, Daniel V, Srivastava A, Jayandharan GR. Nuclear factor (NF)-kappaB and its associated pathways are major molecular regulators of blood-induced joint damage in a murine model of hemophilia. J Thromb Haemost. 2013;11(2):293-306. doi: 10.1111/jth.12101. PubMed PMID: 23231432.

60. Valentino LA, Hakobyan N, Rodriguez N, Hoots WK. Pathogenesis of haemophilic synovitis: experimental studies on blood-induced joint damage. Haemophilia. 2007;13 Suppl 3:10-3. doi: 10.1111/j.1365-2516.2007.01534.x. PubMed PMID: 17822515.

61. van Meegeren ME, Roosendaal G, Jansen NW, Lafeber FP, Mastbergen SC. Blood-Induced Joint Damage: The Devastating Effects of Acute Joint Bleeds versus Micro-Bleeds. Cartilage. 2013;4(4):313-20. doi: 10.1177/1947603513497569. PubMed PMID: 26069675; PMCID: PMC4297157.

62. Frost HM. Wolff's Law and bone's structural adaptations to mechanical usage: an overview for clinicians. Angle Orthod. 1994;64(3):175-88. doi: 10.1043/0003-3219(1994)064<0175:WLABSA>2.0.CO;2. PubMed PMID: 8060014.

63. Teichtahl AJ, Wluka AE, Wijethilake P, Wang Y, Ghasem-Zadeh A, Cicuttini FM. Wolff's law in action: a mechanism for early knee osteoarthritis. Arthritis Res Ther. 2015;17:207. doi: 10.1186/s13075-015-0738-7. PubMed PMID: 26324398; PMCID: PMC4556408.

64. Bove SE, Calcaterra SL, Brooker RM, Huber CM, Guzman RE, Juneau PL, Schrier DJ, Kilgore KS. Weight bearing as a measure of disease progression and efficacy of anti-inflammatory compounds in a model of monosodium iodoacetate-induced osteoarthritis. Osteoarthritis Cartilage. 2003;11(11):821-30. PubMed PMID: 14609535.

65. Clarke KA, Heitmeyer SA, Smith AG, Taiwo YO. Gait analysis in a rat model of osteoarthrosis. Physiol Behav. 1997;62(5):951-4. PubMed PMID: 9333186.

66. Allen KD, Mata BA, Gabr MA, Huebner JL, Adams SB, Jr., Kraus VB, Schmitt DO, Setton LA. Kinematic and dynamic gait compensations resulting from knee instability in a rat model of osteoarthritis. Arthritis Res Ther. 2012;14(2):R78. doi: 10.1186/ar3801. PubMed PMID: 22510443; PMCID: PMC3446452.

67. Liu Z, Hu X, Man Z, Zhang J, Jiang Y, Ao Y. A novel rabbit model of early osteoarthritis exhibits gradual cartilage degeneration after medial collateral ligament transection outside the joint capsule. Sci Rep. 2016;6:34423. doi: 10.1038/srep34423. PubMed PMID: 27756901; PMCID: PMC5069470.